Aerodynamic Analysis-Driven Design and Simulation of a Lift Fan System for Next Generation Fighter Aircraft

By

Muhammad Rishaeel Haider

(Registration No: 00000401485)

School of Interdisciplinary Engineering and Sciences

National University of Sciences & Technology (NUST)

Islamabad, Pakistan

(2024)

Aerodynamic Analysis-Driven Design and Simulation of a Lift Fan System for Next Generation Fighter Aircraft

By

Muhammad Rishaeel Haider (Registration No: 00000401485)

A thesis submitted to the National University of Sciences and Technology, Islamabad,

in partial fulfillment of the requirements for the degree of

Master of Science in

Computational Science and Engineering

Supervisor: Dr. Ammar Mushtaq

School of Interdisciplinary Engineering and Sciences

National University of Sciences & Technology (NUST)

Islamabad, Pakistan

(2024)

THESIS ACCEPTANCE CERTIFICATE

Certified that final copy of MS/MPhil thesis written by Mr Muhammad Rishaeel Haider Registration No. 401485 of __SINES__ has been vetted by undersigned, found complete in all aspects as per NUST Statutes/Regulations, is free of plagiarism, errors, and mistakes and is accepted as partial fulfillment for award of MS/MPhil degree. It is further certified that necessary amendments as pointed out by GEC members of the scholar have also been incorporated in the said thesis.

Signature with stamp: _____
Dr. Ammar Mushtaq
Associate Professor
SINES - NUST Sector H-12
Islamabad

Name of Supervisor: _Dr Ammar Mushtaq_____

Date: ___16th Aug 2024_____

Signature of HoD with stamp: _____
Dr. Mian Ilyas Ahmad
HoD Engineering
Professor
SINES - NUST, Sector H-12
Islamabad

Date: ___20/08/2024_____

Countersign by

Signature (Dean/Principal): _____

Date: ___20/08/2024_____

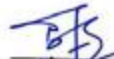## Certificate for Plagiarism

It is certified that MS Thesis Titled <u>Aerodynamic Analysis-Driven Design and</u> <u>Simulation of a Lift Fan System for Next Generation Fighter Aircraft</u> by <u>Muhammad</u> <u>Rishaeel Haider</u> has been examined by us. We undertake the follows:

a. Thesis has significant new work/knowledge as compared already published or are under consideration to be published elsewhere. No sentence, equation, diagram, table, paragraph or section has been copied verbatim from previous work unless it is placed under quotation marks and duly referenced.

b. The work presented is original and own work of the author (i.e. there is no plagiarism). No ideas, processes, results or words of others have been presented as Author own work.

c. There is no fabrication of data or results which have been compiled / analyzed.

d. There is no falsification by manipulating research materials, equipment or processes, or changing or omitting data or results such that the research is not accurately represented in the research record.

e. The thesis has been checked using TURNITIN (copy of originality report attached) and found within limits as per HEC plagiarism Policy and instructions issued from time to time.

Name of Supervisor: Dr. Ammar Mushtaq

Signature & Stamp of
Supervisor:

Dr. Ammar Mushtaq
Associate Professor
SINES - NUST Sector H-12
Islamabad

AUTHOR'S DECLARATION

I Muhammad Rishaeel Haider hereby state that my MS thesis titled "Aerodynamic Analysis-Driven Design and Simulation of a Lift Fan System for Next Generation Fighter Aircraft" is my own work and has not been submitted previously by me for taking any degree from National University of Sciences and Technology, Islamabad or anywhere else in the country/ world.

At any time if my statement is found to be incorrect even after I graduate, the university has the right to withdraw my MS degree.

Name of Student: Muhammad Rishaeel Haider

Date: 20th August, 2024

DEDICATION

I dedicate this thesis to my family, whose unwavering support and belief in me have been my greatest source of strength and motivation. To my parents, for their endless love, sacrifices, and encouragement, and to my siblings, for always being there with their words of wisdom and support. I also wish to express my deepest gratitude to my supervisor, Dr. Ammar Mushtaq, for his exceptional guidance, patience, and invaluable insights throughout this journey. Your mentorship has been instrumental in shaping this work and my growth as a researcher. This thesis is a testament to the collective effort and inspiration from all who have believed in and supported me.

ACKNOWLEDGEMENTS

First and foremost, I would like to express my deepest gratitude Allah Almighty who has made me capable enough to embark on such a journey to make an innovative mark in the industry and academia. Secondly, I would like to express my deep gratitude to my supervisor, Dr. Ammar Mushtaq, for his invaluable guidance, support, and encouragement throughout this research. Your expertise, patience, and constructive feedback have been instrumental in shaping this thesis, and I am profoundly grateful for the opportunity to learn from you.

I am also deeply thankful to my family for their unwavering support and belief in me. To my parents, your endless love, sacrifices, and encouragement have been my foundation, enabling me to pursue my dreams and overcome challenges. To my siblings, your support and words of wisdom have been a constant source of strength and motivation.

I extend my sincere thanks to my colleagues and friends, whose camaraderie and support have made this journey more enjoyable and fulfilling. Special thanks to Hashim Shafiq, Faiq Ahmad, Bilal Ali, Hafiz Muhammad Yasir Bhatti, Bilal Sarwar, Arqam Habib, Muhammad Bilal and Moneeba Bilal for their insightful discussions, collaboration, and encouragement.

I am grateful to the faculty and staff of School of Interdisciplinary Engineering and Sciences for providing a conducive learning environment and for their administrative and technical support. Special appreciation goes to Computational Aeronautics Lab, Dr. Adnan Masood for his assistance and support.

Thank you all for your support and contributions, without which this thesis would not have been possible.

TABLE OF CONTENTS

LIST OF TABLES

LIST OF FIGURES

LIST OF SYMBOLS AND ABBREVIATIONS

VTOL	Vertical Takeoff and Landing
STOVL	Short Takeoff and Vertical Landing
ASTOVL	Advanced Short Takeoff and Vertical Landing
NGFA	Next Generation Fighter Aircraft
JSF	Joint Strike Force
CFD	Computational Fluid Dynamics
SA	Spalart-Allmaras
SST	Shear Stress Transport
GUI	Graphic User Interface
TUI	Text User Interface
CAD	Computer Aided Drafting
UAV	Unmanned Aerial Vehicle
3-BSM	3 Bearing Swiveling Module
RANS	Reynold's Averaged Navier Stokes
DES	Detached Eddy Simulations
ATM	Automatic Topology Meshing
CRF	Counter-Rotating Fan
EDF	Electric Ducted Fan
ANC	Active Noise Control
NMFR	Normalized Mass Flow Rate
PR	Pressure Ratio
RPM	Revolutions Per Minute
$\alpha_1`$	blade inlet angle
$\alpha_2`$	blade outlet angle
θ	blade camber angle $= \alpha_1` - \alpha_2`$
ζ	setting or stagger angle

s	pitch (or spacing)
ε	deflection = $\alpha_1 - \alpha_2$
α_1	air inlet angle
α_2	air outlet angle
V_1	air inlet velocity
V_2	air outlet velocity
i	incidence angle = $\alpha_1 - \alpha_1`$
δ	deviation angle = $\alpha_2 - \alpha_2`$
c	chord
$(\Delta h_0)_{st}$	Enthalpy rise in stage
u	Rotational velocity
$\dot{m}$	Mass flow rate
c_x	Absolute Velocity
A	Inlet/outlet area
d_t	Tip diameter
d_h	Hub diameter
P	Static Pressure
$(\Delta T_0)_{st}$	Total temperature rise in stage
Ψ	Pressure Coefficient

R	Reaction
$(\Delta p)_r$	Pressure rise in rotor
Δp_{st}	Pressure rise in stage
β_2	Relative velocity outlet angle
c_{y1}	Inlet swirling component
w_{st}	Total Stage Work
w_I	Stage 1 work
w_{II}	Stage 2 work
c_3	Absolute velocity at blade 2 inlet
c_2	Absolute velocity at blade 2 outlet
ϕ	Flow Coefficient
$B_x(x)$	X component of quadratic Bezier function
$B_y(x)$	Y component of quadratic Bezier function
θ	Theeta

ABSTRACT

The advancement in the aerospace industry has given much versatile technologies, but they all have their own complications and limitations. The history of Vertical Take-off and Landing (VTOL) aircrafts started with helicopters, then to tilt rotor aircrafts and then to turbo powered machines, but they all had their limitations when it came to their implementation in a fighter aircraft. The main purpose of this research is to design a contra-rotating ducted lift fan for VTOL application in the Next Generation Fighter Aircrafts (NGFA). CFD simulations of an NGFA are performed in ANSYS Fluent at various operating conditions in cruise and VTOL mode to identify lift fan design requirements. RANS with SST k-ω turbulence model was used to perform Cruise simulations at 0.7-0.9 Mach number at 0 to 5 degrees angle of attack. Similarly, for VTOL overset mesh technique of ANSYS Fluent was utilized. Based on CFD simulations, theoretical calculations were performed to obtain blade profile, number of blades, number of stages, and duct diameter etc. The analysis suggested a two stage contra-rotating ducted fan with 50inch diameter designed to achieve 80kN thrust. To achieve 80KN thrust, pressure ratio of 1.9 at 3000 RPM and 204 kg/s mass flow rate was proposed. To test the performance of the proposed lift fan, ANSYS CFX which specializes in CFD of turbomachinery was used. The simulation results showed an excellent agreement with the theoretical design calculations. The proposed two stage contra-rotating lift fan attained 71% efficiency to achieve the design requirements of 80KN thrust with 12% error. The pressure ratios, velocity differentials, swirling, isentropic efficiencies, temperature variations along with density changes were mainly observed for the thrust production of the lift fan unit.

1   INTRODUCTION

Since the time of Wright brothers, the aircraft technology has been going towards versatility and there have been flaws in the aircraft designs which are continuously being improved and improvised in the upcoming generations in order to attain a better efficiency, air superiority, better range, maneuverability, range and performance. One major capability which is crucial in modern aviation is the Vertical Take-off and Landing (VTOL) technology. In the war times, there are multiple constraints which have to be pondered upon since time, location and accessibility are major factors which have to be kept in mind while deploying a suitable aircraft which may be able to overcome all of these factors in order to prove beneficial for the forces. As little time is available to acquire air superiority, the runways may be damaged which may lead to delayed take-offs and may cause damage to the landing gears of the aircraft. Thus, to overcome these sensitive VTOL technology plays an important role specifically in military applications.

In order to replace the three aircrafts, F-16 Falcon, AV-8B Harrier and F/A-18 Hornet, used by the USAF, US Marine Corps and US Navy respectively, by one aircraft with multiple variants, has been the goal since a long time. Therefore, F-35 Joint Strike Fighter (JSF) had been developed with three variants, F-35-A, F-35-B and F-35-C for USAF, US Marine Corps and US Navy respectively. This single aircraft has the capability to fulfill all the requirements having minor changes in these mentioned variants according to their utility.

The F-35-B has state of the art technology, which mainly has innovative module in it that is the Lift Fan System, developed by Rolls Royce Allison, it has the capability to help the aircraft take-off and land in vertical direction, which serves a major role in the aviation industry. Since it is mainly developed for the aircraft carriers and for runways which are practically inaccessible or even for time sensitive operations. Replacing the previous vertical take-off and landing aircraft, the AV-8B Harrier,[1] the F-35-B has a considerable improved ground effect which creates an envelope like flow under the aircraft which provides the necessary lift for the aircraft to take-off and land vertically, while providing the specified thrust-to-weight ratio. Thus, making it the first ever aircraft which has the capability to fly at supersonic speeds, hover like a helicopter and land vertically. Its unique propulsion system has made it stand out from all the 5th generation fighter aircrafts.

The main purpose of this research is to develop a method for designing and simulating a lift fan system. Since there are many complexities associated with blade design therefore a specific approach is acquired in order to go through the whole design process. Because there have historically been a variety of VTOL aircraft layouts depending on the engines and their uses. In the 1960s, this technology became more and more popular thanks to a variety of rotorcraft designs. This includes powered lift aircraft, helicopters, gyrodynes, and tiltrotors. Rolls Royce tilt rotor engines are used in aircraft such as the Boeing V22 Osprey to aid with vertical take-off and landing. This idea was later used to the Lockheed Martin F-35-B.[2] It has a separate lift fan system behind the cockpit that is operational during take-off and landing. This system, along with the roll posts at the wings and the thrust vectoring nozzle, increases the aircraft's ground effects and stability.

The inlet down chooses procedure, the lift fan blade's intricate design, and the ensuing redesign and optimization process are examples of previous research. In addition to the flight test findings, the outcomes of the subscale, full-scale, and inlet pressure recovery tests have been presented.

Dr. Paul Bevilaqua is the mastermind behind this stupendous innovation in the aeronautics industry by proposing the lift fan system just to serve the purpose of STOVL in fighter aircrafts. According to the requirements, the aircrafts can be divided into different designs, each of which serves the purpose accordingly.[3] Helicopters are considered to be a prime example of vertical take-off and landing aircrafts, but these rotorcrafts have very limited usability and functionality. Typically, helicopters are used for short range commute with minimal weight loading and passenger capacity. Also, these lie in the subsonic regime and cannot be operated in dogfights and other supersonic operations.[4] Yet, these can be considered as an inspiration for the current VTOL fighter aircrafts. Along with the helicopters, tiltrotors serve the purpose of short take-off as they work as a helicopter while taking off and function like a conventional turboprop aircraft in cruise flights. V-22 Osprey is the best example of a tiltrotor aircraft, it has a mechanism similar to that of a helicopter mounted on the wings which are directed in vertical direction for the thrust propulsion acting directly towards the ground, during transition the direction of the rotors are changed and comes in line with the flight direction when in cruise.[5]

Figure 1.1 Bell Boeing V-22 Osprey

It also operates in the subsonic regime yet it comparatively has an enhanced range than helicopters. It usually serves the purpose mainly for transporting cargo and military equipment. Another VTOL configuration which was considered includes Tilt wing and Tail sitter, but due to less efficiency and poor pilot visibility, these aircrafts are now not under development by many companies, yet NASA has worked on these aircrafts which in return brought up the manufacturing of GL-10 tilt wing, and Puffin tail sitter.[6] Due to the reduced speeds and range of helicopters and gyrodynes, they are currently not included in VTOL aircraft category.

Powered lift aircrafts have lifting components which help them in vertical take-off and landing, these components usually generate lift greater than the turboprop engines of tiltrotors or the turboshaft engines of helicopters.[5] While taking off, the thrusters are directed downwards providing maximum thrust in the vertical direction which thus helps in the lifting of the aircraft along with other thrust vectoring components. The jump jet AV-8B Harrier was one of the most successful VTOL aircraft but it had a few drawbacks which were crucial to the aircraft structure, as the aircraft had to be dropped from a certain height vertically downwards since it had an adverse ground effect.[7]

To overcome this problem, lift fan system was developed. It mainly includes a set of counter rotating fans which provide thrust in the vertical direction and are driven by a shaft connected to the main engine, with inlet and outlet guide vanes which assist in the thrust vectoring during VTOL and transition as well. Along with the lift fan system which was mainly developed by Rolls Royce, a thrust vectoring nozzle was

also developed in order to provide a constant thrust at the exhaust pointing downwards and the thrust from the lift fan. The Three Bearing Swivel Module serves the purpose of vertical acting thrust as it has the capability of rotating in three degrees of freedom, which later on rotates back in the original position once the VTOL is achieved.[8]
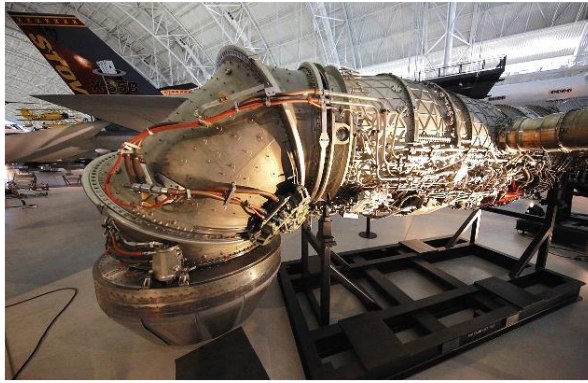
Figure 1.2 Bearing Swivel Module

1.1 LIFT FAN SYSTEM

The F-35-B propulsion system includes a single engine F135-PW-100 developed by Pratt and Whitney with an afterburner along with which it constitutes of three-bearing swivel nozzle, driveshaft which is connected to the main engine, clutch and roll posts.[8] Each of these components have their specific purposes which help in the vertical take-off and landing.
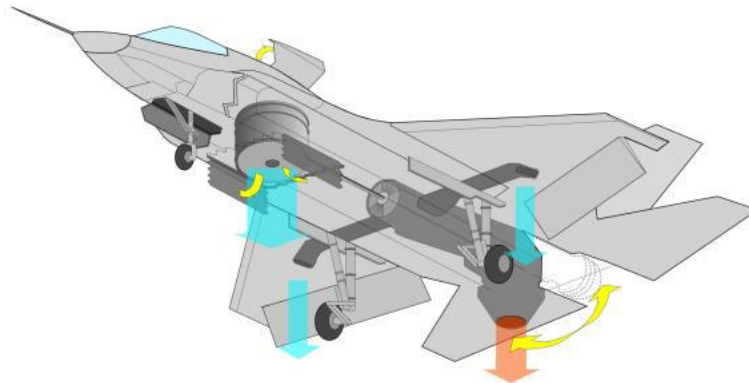
Figure 1.3 STOVL nozzle, lift fan and roll post configuration

During the VTOL, all the thrusters are acting in downward direction, the lift fan and the 3-BSM nozzle provides vertical thrust in longitudinal axis, whereas the two roll posts at the root of the wing provide stability in the lateral axis. This configuration helps in the proper formation of a fountain under the aircraft which eventually helps the aircraft in lifting, furthermore providing better ground clearance as well.
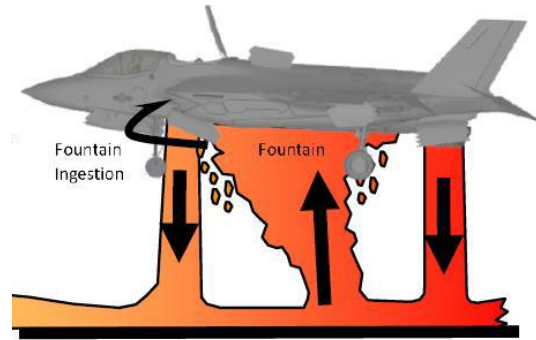
Figure 1.4 Fountain ingestion [9]

The main difference between the conventional takeoff and landing and the carrier variant, which is VTOL is the inclusion of these components. The driveshaft from the low-pressure compressor of the main engine is connected to the lift fan which rotates the rotor blades present inside the lift fan system. The outlet nozzle of the lift fan has a variable vane are which helps in thrust vectoring. This also assists during the transition of aircraft flight from takeoff to cruise and then cruise to landing. [8]

1.1   Ground Testing Program:

Owing to the concerns related to the weight and performance of the driveshaft and the gear box of the lift fan, ground testing was important. Whether the lift fan will be able to withstand the ground effects, the synchronization of the lift fan with the thrust vectoring nozzle of the main engine, and the controlling of the lift fan nozzle are all the parameters which were to be tested during the ground operation. The lift fan consisted of two-stage counter-rotating fan which was driven by two separate gears in order to reduce and distribute the loading on each fan blade set.
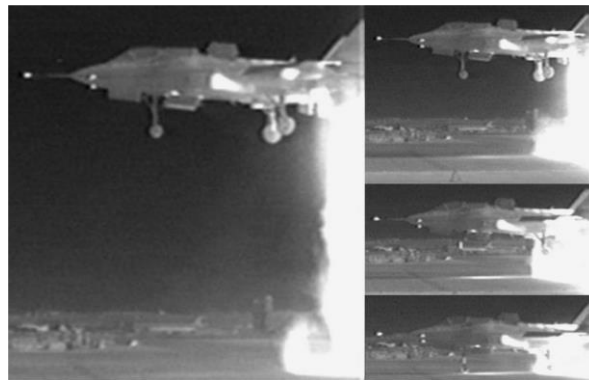
Figure 1.5 Lift fan and Thrust vectoring nozzle testing [10]

The performance of the lift fan was tested under two conditions, the first one was done with no lift fan operating and the second one was done with lift fan operating, this showed a rapid transfer of the thrust shifting from the cruise mode to the VTOL mode which provided the results with pitch control as well. The test was conducted with a full-size aircraft frame which was done in the Pratt and Whitney testing facility.[11]

1.2 Motivation and Research objectives:

1.2.1 National defense and security

PAEC Kamra is working on Next Generation Fighter Aircraft, to catch up to the modern world of Stealth aircrafts. This research will be useful as it covers three different aspects, cruise performance, VTOL mode and lift fan design and simulation.

1.2.2 Industrial and economic development

US has a total investment of 1.3 trillion $ in this single project for the development of VTOL stealth fighter aircraft technology, which later on gave them a marvel of Lockheed Martin F-35B, it has its various capabilities of short takeoff and vertical landing on shorter runways and adverse environments, close air support, reconnaissance and special operations. By the end of this research there would be a fair idea of how to reproduce the Lift fan system for VTOL aircrafts in a better way.

1.2.3 Advantages of VTOL technology

VTOL technology has various advantages which are listed as follows;

- Fighter aircraft can land and take off vertically thanks to lift fan systems, which lessens the need for traditional runways. This feature increases operational flexibility by enabling operations in situations when conventional runways are impractical or unavailable.

- By allowing the aircraft to enter isolated and harsh areas, the incorporation of lift fan systems increases the aircraft's operational reach. This flexibility is essential for a variety of mission scenarios, such as warfare, humanitarian relief, and reconnaissance.

- Fighter aircraft fitted with lift fan systems have the ability to be quickly mobilised in order to react to urgent circumstances. This capacity guarantees prompt response times in emergency situations and improves battle preparedness.

1.3   Objectives

Following are the important listed objectives of the research;

1. CFD analysis of a next generation fighter aircraft at various operating conditions for cruise and VTOL using overset meshing
2. Mathematical modelling and profile generation of the fan blade using Jowkousky Transformation of a two-stage counter-rotating fan.
3. CFD simulation of the designed model to observe the flow behavior and thrust results.

1.4   Thesis Arrangement:

Chapter 1 discusses the introduction of lift fan technology in aircrafts in general. **Chapter 2** includes the discussion of literature review of counter-rotating fans in aircrafts and UAVs. **Chapter 3** discusses the methodology used in the research, which includes design, meshing, CFD setup for cruise, VTOL and lift fan system and the mathematical modeling as well. **Chapter 4** includes the discussion of results of the CFD simulations performed on each case, cruise, VTOL and lift fan. Finally, **Chapter 5** discusses the conclusion of the research done.

2 CHAPTER 2: LITERATURE REVIEW

VTOL has transformed the operational flexibility of fighter jets and UAVs and certainly has played an important role in aviation advancement. This technology makes an aircraft to hover and requires no runway in that it can fragile anywhere inclusive of the cities, forests, and even on ships. The utilization of VTOL technology is most suitable in military use since flexibility and dispatch are significant factors.

Some existing fighter aircraft have incorporated VTOL technology in using it in several modern models. The best example is the F-35B Lightning II of the Joint Strike Fighter group established for the USMC and other partners. The F-35B is fitted with a major power plant that has a two-stage counter-rotating low-pressure turbine fan. This system designed by Rolls-Royce lets the aircraft change from the conventional mode of flight and VTOL mode. The two-stage fan creates vertical lift by directing air downwards while the main engine confers forward speed. This produced design allows F-35B to available for use in short take-off and landing tactical shallow strip, as well as aboard aircraft carriers. [12]

Referring to UAVs, versatility through the means of the VTOL technologies has led to the creation of highly effective drones with multi-dimensional capabilities. The difference is that these UAVs can station keeping, taking off and or landing in small spaces which make them perfect in surveillance, reconnaissance and logistic roles in combat as well as in civil use.[13] The usability of VTOL UAVs can be useful in disaster recovery, a search for people in cities and other situations where conventional, runwayed aircraft can't be effectively launched and used.

The VTOL system on the F-35B is accompanied by a two-stage counter-rotating fan which distinguishes it from other similar systems. It together with the main engine of the aircraft is used to provide the lift that enables a vertical takeoff as well as landing. The particular organization of the propulsors counter rotating decreases turbulence and increases thrust, turning the F-35B in a capable tool of many operational scenarios. Inter-conversion between hover and forward flight is smooth with this system to enable the aircraft to change its flight mode depending on the mission demand.[14]

In a broader context VTOL technology in both fighter aircraft and UAVs is a revolutionary advancement in the area of aviation as it offer unique operating features. Application of such systems as the two-stage counter-rotating fan of F-35B presupposes the identification of the advancements within this sphere.

2.1 CFD Analysis using Hybrid Meshing:

To compare the CFD performance of the VTOL mode, the Lockheed Martin Aeronautics Company developed two CFD codes, Falcon and Tenasi, these are two numerical discretization techniques which comprise of cell-centered and node-centered analysis. The mesh configuration was varied with prism layer included.
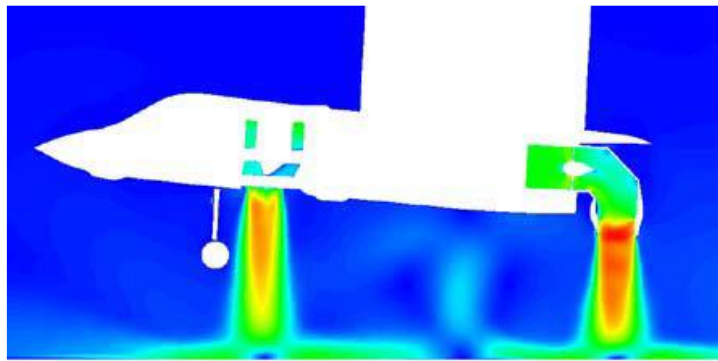
Figure 2.1 CFD analysis of VTOL mode, Side view [15]

Adaptive mesh improved the results for the analysis, which was determined by the comparison of C_p and velocity, later on it was suggested to use better CFD models instead of Reynolds Averaged Navier Stokes, which is Detached Eddy Simulation and Reynold's Stress Model for more effective turbulent study. [16]

2.2 Analytical estimates of the lift fan:

The shaft horse power can be calculated using the momentum energy consideration for thrust and velocity, which has a direct relation with the density of the atmosphere and the area of the lift fan;

$$HP = T\,V$$

Mass flow rate and velocity are important factors of thrust only if the lift fan is considered to be cylindrical, which means that the inlet and outlet diameter of the lift fan are equal;

$$T = \rho V^2 A$$

The thrust produced by the lift fan of F-35-b is around 83kN, which is comparatively significant as compared to that produced by the F/A-18, along with this thrust the thrust from the 3-BSM nozzle is also ranges from 80kN to 83kN. [15]

2.3 Rolls-Royce Jet-Powered Engines:

The key contributors in the development of the lift fans are Rolls Royce along with Pratt and Whitney and Lockheed Martin Skunk Works. Rolls Royce has developed lift fans for several types of takeoff modes including, Vertical takeoff and landing (VTOL), Vertical/Short takeoff and landing (V/STOL) and Advanced short takeoff and vertical landing (ASTOVL), these modes were used in various aircrafts including AV-8A, AV-8B, Yak-38 and the latest F-35-B which was known as X-35-B in the experimental phase.[17] The comparison of the jet type and their year of service along with the number of lift engines are mentioned in the summary below;
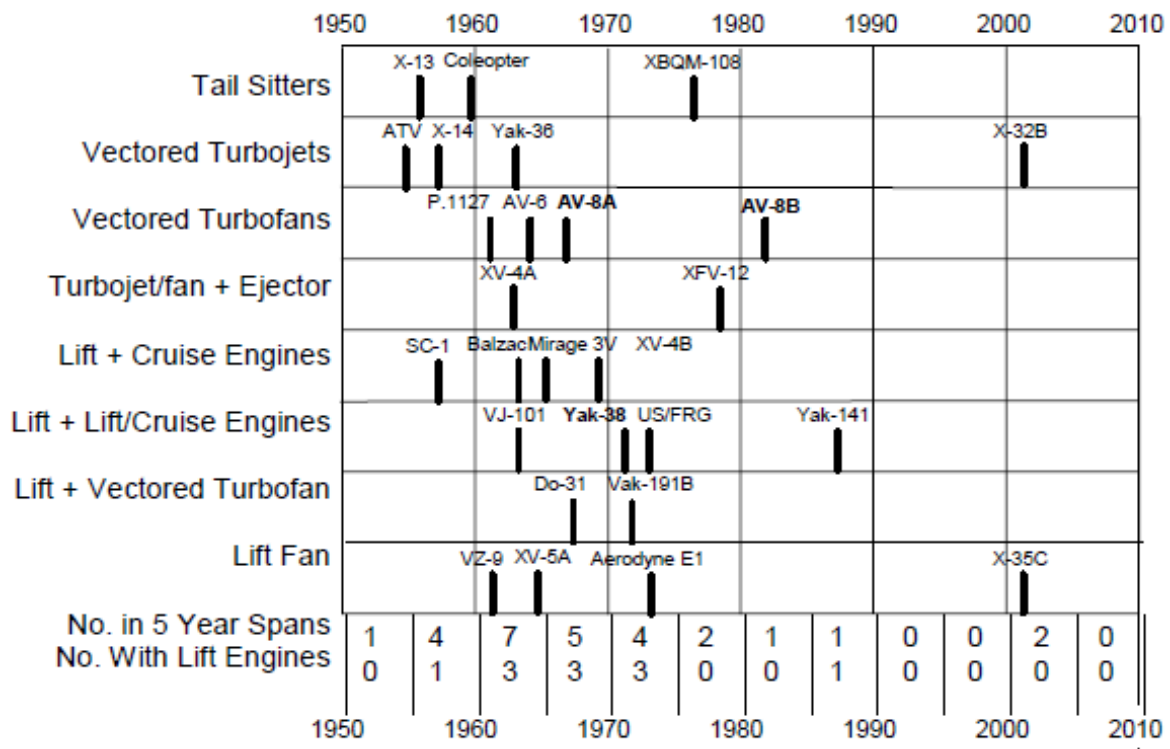
Figure 2.2 Summary for VTOL, V/STOL and ASTOVL aircrafts[17]

As the data sheet provided by the Rolls Royce talks about the performance and operation of the lift fan capable of delivering 20,000 lbf of cold thrust, having a 50-inch diameter of 2-stage

11

counter-rotating fan, whereas the roll posts provide with a total of 1950 lbf bypass thrust from the main engine, along with which the 3-BSM directs a total thrust of 18,000 lbf from the main engine.[17] The main purpose of the lift fan is to provide thrust more than the weight of the aircraft in order to lift which is directed downwards at zero flight speed which later on is transitioned to the aircraft cruise flight.[18]

The lift fan system is no doubt an aviation marvel, pushing the aeronautics to its limits in the development and operation. Even though its production cost has been over the skies yet the aircraft contains the maneuverability and stealthiness equivalent to the F-22 Raptor which serves a key role.[19] Despite the efforts of the developers, several models were made including the advanced vectored thrust, tandem fan, ejector lift and remote augmented lift system, the lift fan system came out to be a more efficient and practical than the other proposed models.[20] The CFD simulations were also performed in order to analyze the flow effects on different transonic conditions at different angle of attack in order to optimize the design of the wing and body, keeping the stealthiness of the aircraft in account.[18]

2.4   Counter-rotating fan in manned aircrafts

Counter-rotating fans (CRFs) for both civil and military applications is quite impressive. They designed two different fan types, one with a low bypass ratio suitable for commercial aircraft, and another with a high bypass ratio ideal for military jets. The study thoroughly explores how these fans perform under various conditions using advanced computational methods.

The methodology is robust, combining different analytical and computational techniques. For instance, they used CFD simulations to examine the flow characteristics and performance metrics like pressure ratios and efficiencies. The civil fan design prioritized low fuel consumption and noise, achieving a remarkable efficiency of over 91%. On the other hand, the military fan, designed for high-speed applications, managed to maintain efficiency and performance even under more demanding conditions.[21]
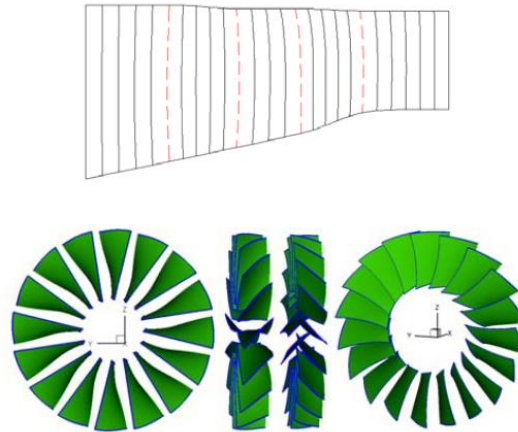
Figure 2.3 Flow paths of front and back counter-rotating fan[21]

One of the standout aspects of the work is how they addressed shock losses, particularly in the aft rotor, which is critical to the overall fan performance. The design tweaks they implemented, especially for the military fan, to handle these shocks while ensuring the structural integrity of the blades are noteworthy. This careful attention to both aerodynamic and structural factors showcase the depth of their research.[21] The research provides valuable insights into the design and performance of CRFs, highlighting the potential advantages in different aviation contexts. The study's findings could significantly influence future fan designs, making them more efficient and effective for both commercial and military applications.

2.4.1   Numerical Study on small Contra-Rotating fans

The development of small contra-rotating electrical ducted fan engines. The researchers have done an excellent job combining experimental tests with advanced numerical simulations to evaluate the performance of these engines.[22]
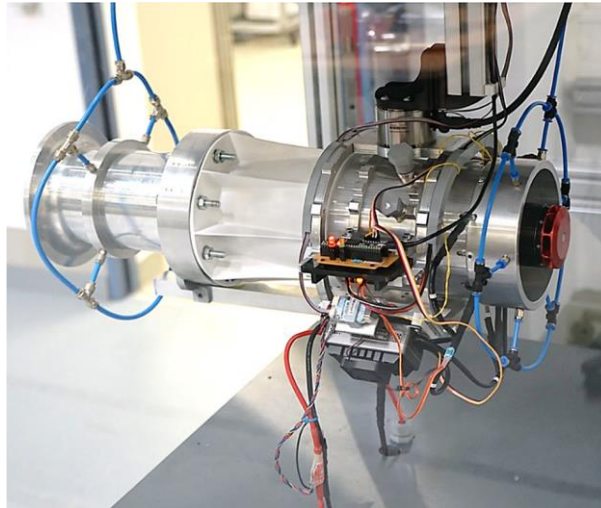
Figure 2.4 Fully Functional contra-rotating fan[22]

Their work is particularly significant given the growing interest in electric propulsion systems for aviation. By using two independently controlled brushless motors to drive the rotors, they have demonstrated a flexible and efficient design that can adapt to various operating conditions. The experimental results show that the engine operates smoothly and efficiently, though motor heating is an issue that needs addressing. The numerical simulations provided a detailed understanding of the flow characteristics within the engine, and the good agreement with experimental data validates their approach.[22] However, the study also highlights the challenges in accurately modeling all physical phenomena, such as heat transfer from the motors. Overall, this research contributes significantly to the field of electric propulsion, showing that contra-rotating designs hold promise for future aviation applications. The combination of compactness, efficiency, and the ability to operate at high thrust levels makes these engines a promising solution for various aerospace needs.

2.4.2 Aspirated Counter-rotating Fan

The rigorous design process and innovative use of aspiration have shown that it's possible to achieve high-efficiency, high-pressure ratio fans suitable for advanced aircraft propulsion systems. The methodology employed, combining advanced aerodynamic and mechanical design with thorough testing in a blowdown facility, ensures that the results are both accurate and practical. The aspiration technique, which helps manage shock and boundary layer losses, is particularly noteworthy and represents a significant advancement in fan design.
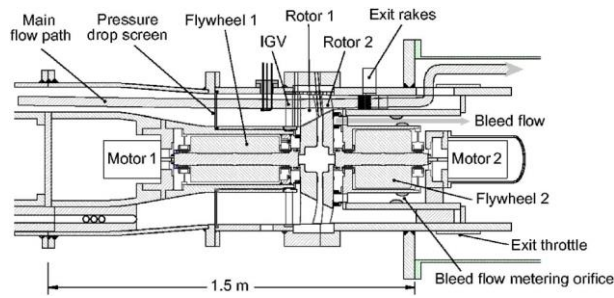
Figure 2.5 Test section of the counter-rotating fan

The findings indicate that counter-rotating fans with aspiration can achieve high levels of efficiency and performance, even under challenging conditions. The research lays the groundwork for future developments in high-performance, compact fan designs for both commercial and military aviation applications. Overall, the study provides valuable insights and practical solutions for designing and testing advanced counter-rotating fans, making it a noteworthy addition to the literature on modern aircraft propulsion systems.

2.5 Counter-rotating fan in UAVs

The research presents a compelling case for counter-rotating fans (CRFs) as a future aircraft propulsion system. By integrating advanced experimental techniques and numerical simulations, the study provides a thorough understanding of the aerodynamic, aeroelastic, and aero-acoustic properties of CRFs.[23] The experimental investigations at DLR's state-of-the-art facilities revealed that CRFs could significantly improve fuel efficiency and reduce emissions compared to conventional engines. The swirl-free exit flow achieved by CRFs is a key factor in their enhanced efficiency, making them a promising alternative for future high-bypass engines.
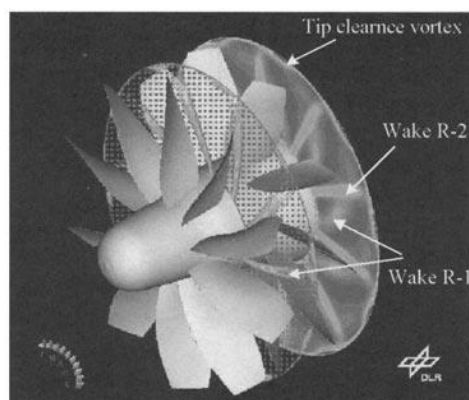
Figure 2.6 Axial positioning of the counter-rotating fan[23]

The study's numerical simulations complemented the experimental data, offering insights into the complex interactions between the counter-rotating rotors. The use of fluid-structure coupling for aeroelastic simulations was particularly noteworthy, providing a detailed picture of blade dynamics under various operating conditions. One of the standout aspects of the research is the successful application of active noise control (ANC) techniques. By reducing fan noise by up to 25 dB, the study highlights the potential of ANC to address one of the major challenges in modern aviation—noise pollution.[23]

Overall, a solid foundation for the future development of CRFs, showing that they hold significant promise in terms of efficiency, performance, and noise reduction. The research is a valuable contribution to the field of aeronautics and could influence the design of next-generation aircraft engines.

2.5.1 Contra-rotating Ducted Fan

A detailed and methodical approach to designing contra-rotating ducted fans for UAVs. The research provides a thorough analysis of the aerodynamic and thermodynamic aspects, ensuring that the design meets the specific thrust requirements while maintaining high efficiency.[24]

The work stands out due to the meticulous design process, which includes a combination of theoretical calculations, numerical simulations, and iterative adjustments. By considering various design parameters and conducting a comprehensive survey of existing technologies, they have developed a robust design that addresses the unique challenges of UAV propulsion.
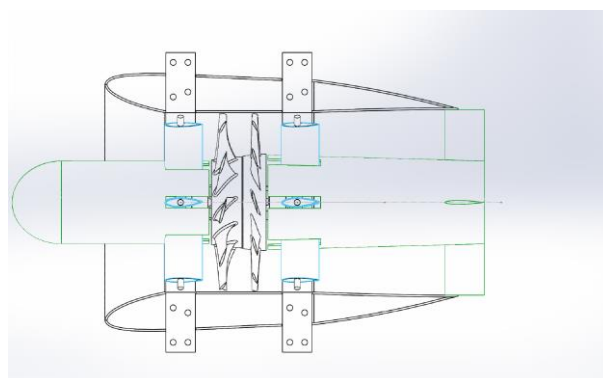
Figure 2.7 Cross-Section of ducted fan[24]

2.6 Effect of Rotor Spacing

One of the highlights of the study is the custom airfoil design, which optimizes the duct and lip geometry to reduce flow separation and enhance overall performance. This attention to detail in the aerodynamic design significantly contributes to the efficiency of the ducted fan. Overall, this research provides valuable insights and a solid framework for developing advanced propulsion systems for unmanned applications. The combination of theoretical rigor and practical considerations makes it a noteworthy contribution to the field of UAV design.[24]

Kim and colleagues' study offers valuable insights into optimizing the design of counter-rotating ducted fans for UAVs. By meticulously analyzing the effects of rotor spacing and duct diffusion angles, they have identified configurations that significantly enhance thrust and efficiency.

Their use of advanced numerical simulations, validated against experimental data, provides robust evidence supporting their findings. The research shows that a rotor spacing of 200 mm and a duct diffusion angle of 0° are optimal for maximizing thrust and the figure of merit. These results are crucial for designing more efficient propulsion systems for UAVs, which require high thrust and maneuverability.[25]
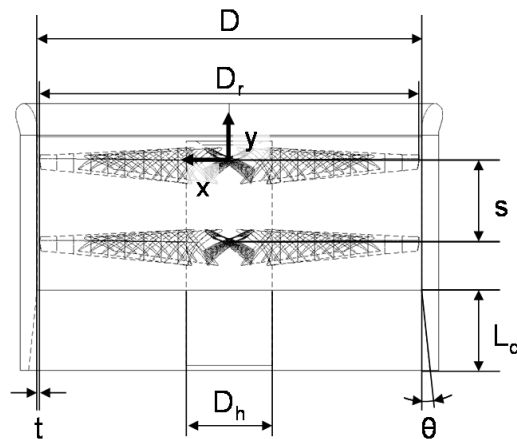
Figure 2.8 Schematic Diagram of Counter-rotating Fan[25]

One of the standout aspects of this study is its practical implications for UAV design. The findings suggest that adjusting rotor spacing and duct angles can lead to substantial improvements in performance without major changes to the overall design. This flexibility is

particularly beneficial for the evolving demands of UAV applications in various fields, from military to civilian uses.

2.7 Experimental Study of Contra-Rotating Lift Fan

Overall, this paper contributes significantly to the field of aerodynamics and UAV propulsion, providing a clear path for future research and development in optimizing ducted fan designs.

Deng and Ren's study provides insightful data on the aerodynamic performance of ducted contra-rotating lift fans for UAVs. Their meticulous experimental approach sheds light on the complex interactions within the contra-rotating mechanism and its impact on force production.

Their findings reveal that while contra-rotating fans enhance lift, they do not double the force generated by single rotors, suggesting room for optimization. The quadratic increase in lift with RPM highlights the unsteady nature of the flow, indicating that traditional steady-state models may not fully capture the dynamics at play.[26]

One of the study's significant contributions is its examination of the ground effect, showing a substantial increase in lift as the UAV nears the ground. This effect, coupled with the observed unsteady flow, provides critical insights for designing more stable and efficient UAVs.

Overall, this research offers valuable guidance for improving the design and performance of ducted contra-rotating lift fans, making it a notable addition to the field of UAV aerodynamics. The detailed methodology and comprehensive analysis presented by Deng and Ren serve as a solid foundation for future studies and design optimizations in this area.[26]

3   METHODOLOGY

The design of a lift fan system for a VTOL aircraft requires a thorough approach and a systematic approach for the blade design for a counter-rotating fan and the CFD simulations. Initially the literature review was done separately on the CFD of the VTOL aircrafts and UAVs, for various cases in which the performance and the integration of the lifting unit in the aircraft was done. The literature also included the identification of design parameters along with performance parameters required for the design of the blade unit. The experimental data of various machines was also observed for the design purpose, but the challenging part was that not much design data was available for a counter-rotating fan of a fighter aircraft, due to which different approaches were merged in order to obtain a suitable design for the lifting unit.

The first phase of the thesis includes learning of CFD techniques which was used for the visual validation and comparison of the F-35-B look alike model in cruise and VTOL mode. A simple rectangular domain was made for the CFD of the aircraft in transonic cruise mode, where the effects of velocity and pressure distributions were observed at different angle of attacks. Secondly the VTOL mode was simulated using CFD technique using the overset meshes for a single degree of freedom under the influence of gravity. Two separate domains were made and later on append into each other in order to visualize the model for take-off condition. This was also a part of visual validation because not enough literature was available for this specific case along with a guess aircraft model.

The main purpose of the cruise and VTOL CFD was to identify the main purpose and idea of a lifting fan unit, specifically for a Next Generation Fighter Aircraft (NGFA). Therefore, in order to identify the research gap this was identified that the literature for the design of lift fan system is not enough, therefore the unavailability of the literature became the research gap and thus to design a whole lifting fan was a challenging task.

The first phase of the design includes the mathematical modelling of the blade, which includes the calculation of velocity triangles, performance parameters and design parameters, which includes the calculations of velocity and pressure components at the inlet and outlet of each stage. A MATLAB code was formed in order to calculate the above-mentioned parameters using the equations of the counter-rotating fan blade. Moreover, the design parameters were

late on used to generate the blade profile. A Bezier curve function was used to make the camber line of the 2-D profile. Then the pressure side and suction side curve was generated using the equations from the design book. An inhouse code was used in order to generate the profile curves of the blade.

The 2-D profile was then imported in the ANSYS Design Modeler, where the profile was used to generate a 3-D blade which was then transformed into the rotor. Thus, a single stage comprised of two rotors which were aligned in opposite directions which rotated in opposite direction. Same orientation was used for the second stage of the rotor which operated at the same rotational speed as that of the first stage. Thus, the two-stage counter rotating fan CAD modelling was completed and was ready for meshing. The meshing was performed in ANSYS TurboGrid, where the structured meshing was performed using the Automatic Topology Meshing (ATM). This is an effective method which helps in developing the structured meshing with better orthogonal quality and skewness, which eventually produces better results.

The CFD analysis was performed in ANSYS CFX, the machine properties were set and the blade sets were assigned separately. The main purpose of the research is to find out the thrust of the designed machine, therefore this must produce a mass flow according to the design point at the operating pressure condition. Later on, the CFD simulations were performed at various rotational speeds and varying outlet pressure conditions in order to find out the surging point and the maximum pressure ratio attained.

Finally, the results were compiled and observed along with thrust performance. CFD contours and swirling of the flow path along with other flow physics was also observed.

3.1 CAD Cleaning

Since the aircraft acquired was not an exact geometry with sizing, airfoil shape and fuselage geometry according to the required F-35-B model therefore the geometry needed to be cleaned of extra and unwanted surfaces. The cleaning process included geometrical correction which further included gap correction, missing surfaces generation and correction of inexact edges and duplicate faces. Since the geometry had sharp edges, it was ensured that they may not be a problem for meshing therefore those were also cleaned. This cleaning process enhanced the CFD results which was important since small and unwanted surfaces provide unwanted results and makes the meshing and CFD computationally expensive.

Component	Dimension
Fuselage	15.9 m
Wing Span	12.43 m
Height	4.7 m

The CAD cleaning process included two geometries of same aircraft, one in cruise mode and the other in VTOL mode. The VTOL mode configuration had landing gears retracted and the lifting fan hood was open along with the downward directed 3-Bearing Swiveling Nozzle. Following shows the geometry for cruise mode.
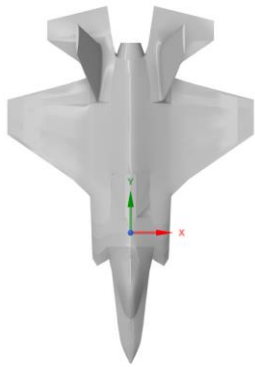
Figure 3.1 Top View
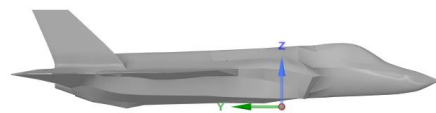
Figure 3.2 Side View
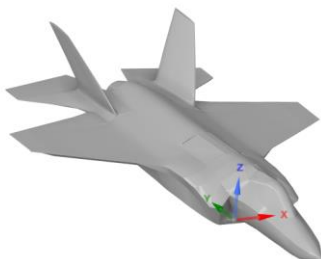
Figure 3.3 3-D view
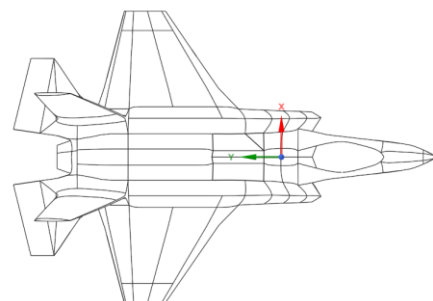
Figure 3.4 Wireframe

Following shows the geometry for VTOL mode of the NGFA.
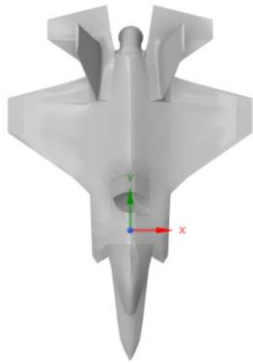
Figure 3.5 Top View
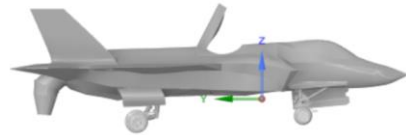
Figure 3.6 Side View
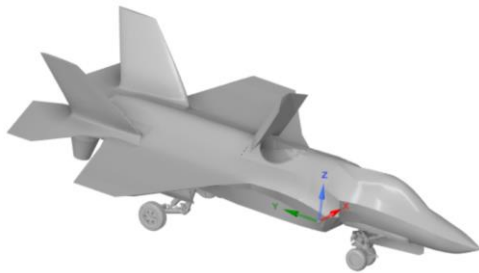
Figure 3.7 3-D View
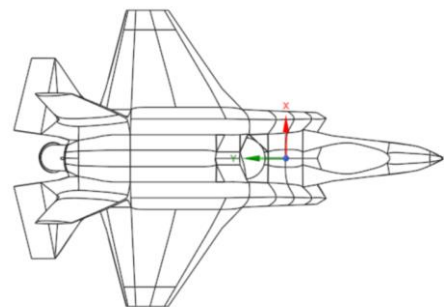
Figure 3.8 Wireframe

3.2   Meshing

A high-quality mesh is often required in order to observe the flow physics over the computational domain. Either a structured or an unstructured mesh may be made but due to the complexity of the geometry, unstructured mesh was preferred. ANSYS Mesh was used in order to make the meshes of the cruise case and the VTOL case. The cruise mesh was made with and

without the viscous sublayer for the transonic mode at the cruise height, but due to the complexities of the geometry the viscous sublayer was subtracted from the aircraft mesh.

3.2.1   Cruise meshing

Mainly the compressibility effects were to be observed during the simulations, therefore the selection of an appropriate domain and appropriate sizing was preferred. Initially the mesh was developed with the viscous sublayer in order to capture the boundary layer effects, but due to sharp edges and small surfaces it was very difficult to capture some areas for the boundary layer. Thus, the mesh was formed without the viscous sublayer.
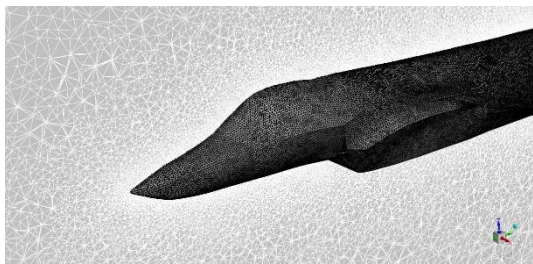
Figure 3.9 Mesh at the nose of aircraft
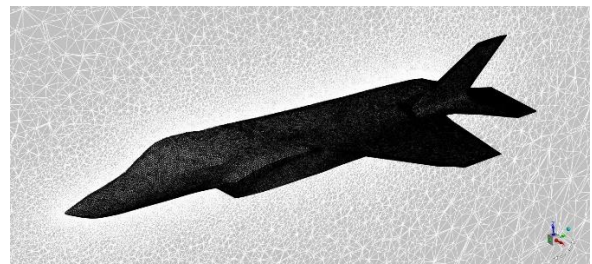
Figure 3.10 Mesh at aircraft body
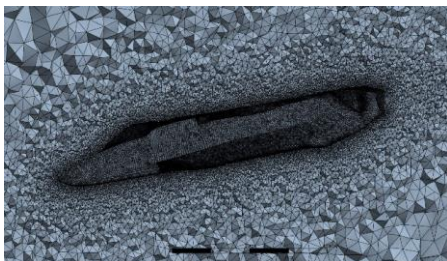
Figure 3.11 3-D Mesh Elements
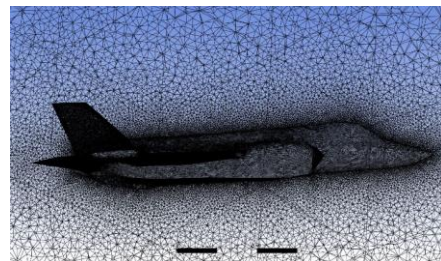
Figure 3.12 Wireframe Mesh Elements

A computational domain of 50L upstream and 100L downstream was made, the mesh was kept dense around the aircraft surfaces which was to capture the high pressure and velocity regions over the aircraft, since the aircraft was reaching the compressible regime and since the compressibility effects are much higher in the transonic regimes therefore a fine computational domain was preferred.

Table 3-1 Mesh information of the cruise domain

	Number of Nodes	Number of Elements

Fluid Domain	9062248	1590262

3.2.2   Overset meshing

For the VTOL case the mesh was made separately for the outer domain and the inner domain. The mesh elements for the outer domain were kept coarse in order to reduce the computational efforts, but for the inner domain containing the aircraft, the mesh sizing was kept fine. The same size as that of the cruise case.
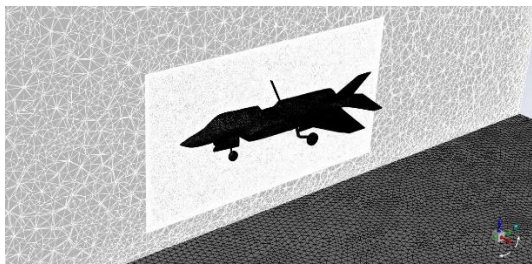
Figure 3.13 Overset mesh domain
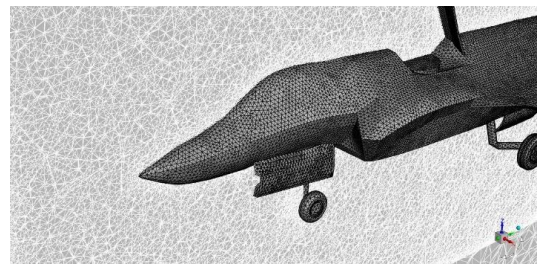
Figure 3.14 Mesh at nose
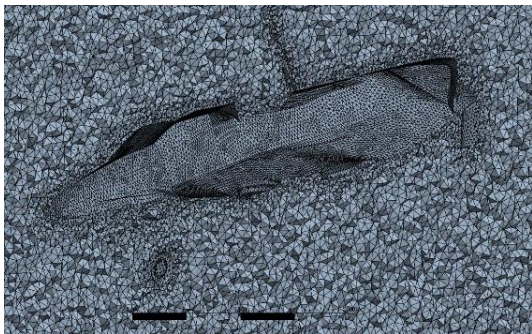
Figure 3.15 3-D mesh elements
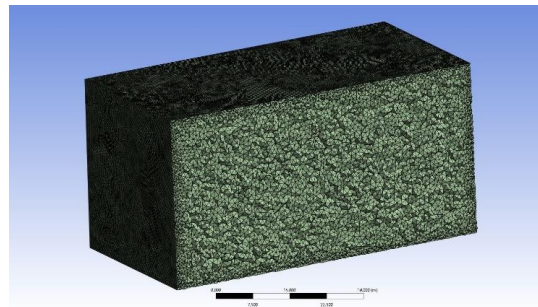
Figure 3.16 3-D mesh elements in outer domain

The outer surface of the inner domain was named as overset as this had to be append in the outer domain, where the dynamic conditions were given in order to visualize the VTOL effects of the aircraft.

Table 3-2 Mesh information of VTOL case

	Number of Nodes	**Number of Elements**
Overset	518378	2847135
Outer Domain	1998217	11048690
Total	2516595	13895825

3.3 CFD Setup

In order to solve the flow physics various CFD techniques may be used, initially the model selection is done. For Reynold's Averaged Navier Stokes (RANS) modelling k-ε, k-ω or Spalart-Allmaras (SA) model is used, all three have their significance in capturing the flow physics. RANS models mainly solve the Navier Stokes equations over the grid which calculates the fluctuations and then averages the solution for modelling. As the name suggests, the solutions are averaged over the grid for modelling in RANS. k-ε and k-ω are both two equation turbulence model which evaluates the kinetic energy and the energy dissipation, these allow to capture the boundary layer effects with much accuracy as well.[27] The k-ω model is mainly used for volumetric flows which is much suitable for compressible flows at high Mach numbers which allows the results to be solved at better accuracy. The SA model is a single equation model which is comparatively less computationally expensive, this is also suitable for external and internal turbulence flows.

While solving the models it is compulsory to have a suitable computational domain along with accurate boundary conditions for the convergence of the solution residuals. Various factors must be considered while solving CFD problems, such as the correct usage of the solvers, multi-grid cycles, convergence criteria, model selection, boundary conditions and the fluid properties. Finally setting the number of iterations for better convergence of the residuals in order to have minimum error.

3.3.1 CFD for cruise

For the cruise case, pressure-based solver was used since it is suitable to use this solver for flows under 1 Mach number, whereas the k-ω SST (Shear Stress Transport) turbulence model

was used since it solves volumetric and external flows much better. The fluid properties were set for the cruise conditions, which included the density of the fluid, dynamic viscosity, temperature, reference pressure, coefficient of pressure at the cruise altitude. For the cruise CFD case an inlet velocity and pressure outlet boundary conditions were set. The velocity range was in the transonic regime, and the analysis was performed at 0.7-0.9 Mach number at 0 to 5 degrees angle of attack. Various cases were observed in order to visually validate the CFD process in comparison to the CFD analysis of the Lockheed Martin F-35-B.

Since the case is operating in the compressible regime, the air as an ideal gas was used, while setting the appropriate values for dynamic viscosity, coefficient of pressure and the temperature at 15,000m (50,000ft).[27] After setting the fluid properties at the cruise altitude and the boundary conditions, the Coupled solver was used since it provides with pressure and velocity coupling, since it captures the flow properties and the thermal effects in a better manner, the solution in the coupled solver solves the Navier Stokes equations in a simultaneous manner, which helps the solver to accurately perform at each iteration. Finally, the convergence criteria were set for the continuity, momentum and energy equation and the iterations were performed.

3.3.2   CFD for VTOL

Initially the outer static mesh domain was given wall condition on the bottom surface and pressure outlet at all the other surfaces in the cuboid domain, whereas for the inner domain containing the aircraft, the outer wall was named as overset in order to enable the overset option.[28] Both the meshes were imported in the fluent having the double precision option active. Pressure based solver was used along with transient conditions under the influence of gravity. The fluid properties were kept as default since the aircraft takes-off at sea level having ambient conditions. The gravitational value was considered to be $9.8m^2/s$. Velocity inlet conditions were given to the lift fan outlet, nozzle outlet and the roll posts as well. Following shows the data for the values which were given as the boundary conditions of the VTOL case.

Table 3-3 Boundary conditions of the VTOL case

Component	Value	Diameter	Temperature	Velocity
Nozzle Thrust	80,000 N	Variable	1100 K	300 m/s
Lift Fan Thrust	80,000 N	1.27m	404 K	226 m/s

| Roll Post Thrust | 14,600 N | 0.3m | 404 K | 205 m/s |

In order to find out the total time required; the second equation of motion was used;

$$S = vt + \frac{1}{2}at^2$$

The aircraft has to be lifted at around 7 meters, the initial velocity of the aircraft is zero since the aircraft is at rest, and the acceleration came out to be 2.489m/s^2 exhaust the total time taken for the liftoff will be 2.372s. thus to find out the time-step size for the transient simulation, the Courant-Friedrichs-Lewy (CFL) condition taken into consideration;

$$C = \frac{v\Delta t}{\Delta x}$$

Δt is the time step size and Δx is the minimum mesh length, therefore for $C = 1$, the time step size comes out to be 0.005. The total number of timesteps come out to be 474 for 2.372s simulation. The simulation took around 28.44 CPU hours for completion having 20 iterations per time step. The case and data file were reported at every timestep for post processing, since the mesh file and data file both were changing because of the lifting of the aircraft. The video file of the simulation was also written, which resulted in more consumption of the computation resource as the Fluent Graphical User Interface (GUI) was used instead of Text User Interface (TUI).

3.4   Validation for ducted fan

The electric ducted fans are suitable for small UAVs in order to reduce the greenhouse gases from the conventional engines, since this small propulsion unit produces a high thrust to weight ratio. These provide higher efficiencies which directs the airflow in a much better manner while directing in a straight direction. An EDF was developed in Computational Aeronautics Lab, the design is optimized and it has the capability to provide around 20N of thrust. The results of the EDF were validated with experimental results. The model was designed in CF-Turbo and then optimized using CFX for CFD simulations.

3.4.1   Geometry of ducted fan

The CAD model was made on CF-Turbo, it is a low fidelity software which requires initial design parameters and makes a preliminary CAD model. A small scale EDF has to be designed

in order to produce 20N of thrust operating at 25000RPM having a low rate of 0.5 m³/s. The initial design parameters were given as an input in CF-Turbo which gave a initial CAD model.

Following are the design parameters which were used for the design procedure;

Table 3-4 Performance parameters of ducted fan

Design flow rate, (m³/s)	0.5
Rotational speed, (rpm)	25000
Total pressure difference	2500
hub-tip ratio	0.5
Number of rotor blade	15

Following were the design parameters which were used to generate the CAD model;

Table 3-5 Design parameters of ducted fan

Parameters	Dh	Ds
Diameter (mm)	60	120
Inlet Flow Angle (deg)	36.9	20.57
Outlet Flow Angle (deg)	48.564	22.29
Axial Velocity (m/s)	58.97	58.97
Tangential Velocity (m/s)	78.53	157.07
Airfoil Type	NACA65-010	NACA65-010
Chord Length (mm)	22	14.9
Stagger Angle (deg)	40	25

Finally, a cad model was obtained having a blade profile of NACA65-010, later on the cad was exported as profile points and curves for meshing in ANSYS TurboGrid.

3.4.2 Meshing on TurboGrid

The CAD profile was imported in ANSYS TurboGrid for meshing. TurboGrid is a specialized software to perform structured meshing on rotary models, specifically or turbines, compressors, fans, either radial, axial or mixed flow machines. The mesh is generated according to the flow path while having defined boundary conditions of the setup, it recognizes automatically the topology of the rotary domain and assigns the interfaces, walls, blades, inlets and outlets and then performs the Automatic Topology Meshing (ATM). This ANSYS module is capable of making high quality structured meshing on highly complex geometries.
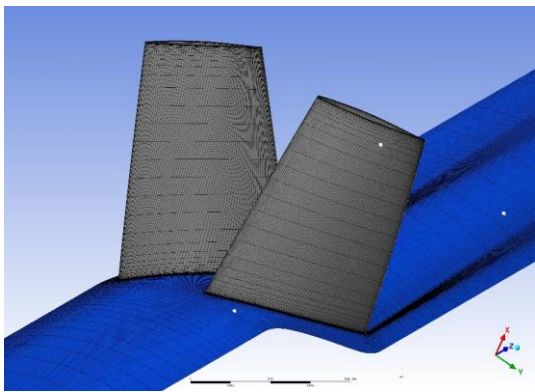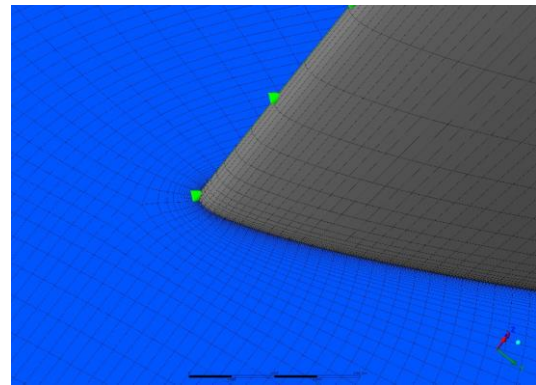

Figure 3.17 3-D blade row mesh

Figure 3.18 Zoomed mesh at blade Leading edge

Following is the mesh topology at 0.5 span of the blade for the single rotor ducted fan, and the number of nodes and elements are as follows

Table 3-6 Mesh information of the ducted fan

	Number of Nodes	**Number of Elements**
Rotor Passage	477315	446292

3.4.3 CFD simulations on CFX

CFD simulations were performed on ANSYS CFX, it is a high-fidelity tool for simulating rotating machines, its robustness and accuracy is much suitable for the simulations of turbomachinery components.

The rotational speed given to the case was 25000RPM having pressure inlet and pressure outlet boundary conditions. k-ω SST RANS model was applied for this specific case having periodic boundary conditions at one passage of the rotor. Constant air density was applied in the fluid properties. And the case was simulated till convergence of 1×10^{-4}.

3.5 Mathematical modelling for blade

Fans have a wide range of applications in commercial, industrial and defense purposes. The main function of a fan is to move gases at a specific speed by increasing the gas pressure. The main configuration of a fan includes, hub, impeller and a shroud casing, mainly the impeller is driven either by an electric motor or in case of an aircraft engine, it is driven by the low-speed turbine stage. Fans can either be axial, radial or mixed flow type, mostly low-pressure fans are axial in which ducted geometry is also included, whereas the high pressure are of radial type. But in the case of flow rates, axial machines have much higher flow rates as compared to the radial machines, due to these reasons the axial machines must have higher number of stages in order to achieve high pressure ratios. In aircrafts these provide with an increase in the velocity of air which directs the flow at a specific angle in the first compressor stage. Whereas in case of VTOL aircrafts, lifting fans help in taking-off, maneuvering using thrust vectoring and hovering, for hovering the fan moves a high amount of fluid directing downwards which helps the aircraft to take-off. The design of the fan has to be efficient in order to keep providing specific amounts of thrust for lift-off.

3.5.1 Initial parameter discussion

There are several aerodynamics and design parameters which are to be considered which include, velocity components which are, absolute, relative and tangential, at inlet and outlet of each rotor having axial and radial components, temperature at inlet and outlet, enthalpy change, density at inlet and outlet since the case is compressible, mass flow rate, volume flow rate, stage pressure coefficients, velocity angles which include absolute and relative, static pressure rise, total pressure, dynamic pressure, pressure difference and ratio, duct diffusion ratio, power

input and gas constant. The design parameters include, hub and shroud diameter, hub and shroud ratio, cross-sectional area, number of rotations, stagger angle, incidence angle, number of stages, number of blades, blade length, chord length, blade twist, pressure head, efficiency, blade profile and several other parameters.

3.6 Performance Parameters

In order to design a lift fan, several design parameters and aerodynamics parameters have to be considered at specific design requirements. The rotor of a fan consists of various number of blades which are attached to the hub. In the case of a VTOL lift fan system, a ducted fan is installed in the fuselage of the aircraft, in which the rotor is covered by a cylindrical casing. The exhaust nozzle of the lift fan is basically a thrust vectoring variable area vane box.

3.6.1 Stage Work

In order to discuss some general parameters, finding out the velocity triangles is necessary, but before that the stage work parameters have to be calculated. The stage work is derived from the Euler's turbine equation which is given as;[29]

$$w_{st} = u\,(\,c_{y3} - c_{y2})$$

Since the flow is adiabatic therefore the work input is in the form of stagnation enthalpy which is expressed as;

$$(\Delta h_0)_{st} = w_{st} = u\,(\,c_{y3} - c_{y2})$$

The mass flow rate through the fan is represented as

$$\dot{m} = \rho A c_x$$

$$\dot{m} = \rho\frac{\pi}{4}(d_t^2 - d_h^2\,)c_x$$

The power required to drive the shaft is given by[29]

$$P = \dot{m}\,(\Delta h_0)_{st} = \dot{m}\,c_p(\Delta T_0)_{st} = \dot{m}u\,(\,c_{y3} - c_{y2})$$

3.6.1.1 Stage Pressure Rise and Coefficient

For isentropic flow,

$$(\Delta h_0)_{st} = \frac{1}{\rho}(\Delta p_0)_{st}$$

Thus, it can be written as,[29]

$$(\Delta p_0)_{st} = \rho u \left(c_{y3} - c_{y2} \right)$$

For stage pressure coefficient,

$$\psi = \frac{(\Delta p)_{st}}{\frac{1}{2}\rho u^2}$$

This pressure coefficient can either be based on static or stagnation pressure.[29]

3.6.1.2 Reaction

Stage reaction is the ratio of static pressure rise in rotor to the stagnation pressure rise in the whole stage, which is represented as,

$$R = \frac{(\Delta p)_r}{(\Delta p_0)_{st}}$$

$$R = \frac{1}{2}(1 - \phi\tan \beta_2)$$

Usually, the degree of reaction ranges from zero to unity.[29]

3.6.2 Velocity Triangles

While finding out the velocity triangles, it is important to assign the inlet and outlet numbering of the rotors and stages respective of their positioning in the machine. Since the design of the lift fan includes a two-stage counter-rotating fan, therefore the initially the mass flow of 204kg/m3 was considered as an initial parameter about which the whole blade design is dependent. Following figure shows a typical ducted counter-rotating fan stage with inlet and outlet support vanes and two rotors which rotate in opposite direction with respect to each other.
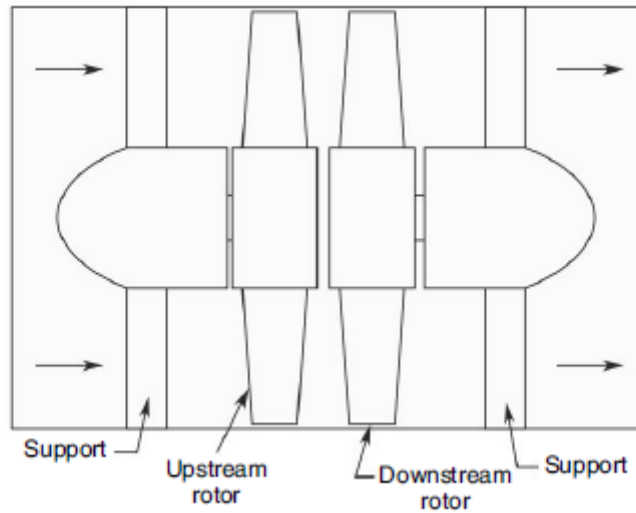
Figure 3.19 Counter-Rotating fan schematic diagram[29]

Figure shows the velocity triangles at the inlet and outlet of both the rotors subsequently, the inlet of the first blade is numbered as 1, and the outlet of first blade and the inlet of the second blade as 2 and 3 respectively, and finally the outlet of the second blade as 4, w and beta are the relative velocity and angle, whereas c and alpha are the absolute velocity and angle.[29] Both the rotors are assumed to have the same rotational speeds therefore the axial velocity is constant throughout the stage.
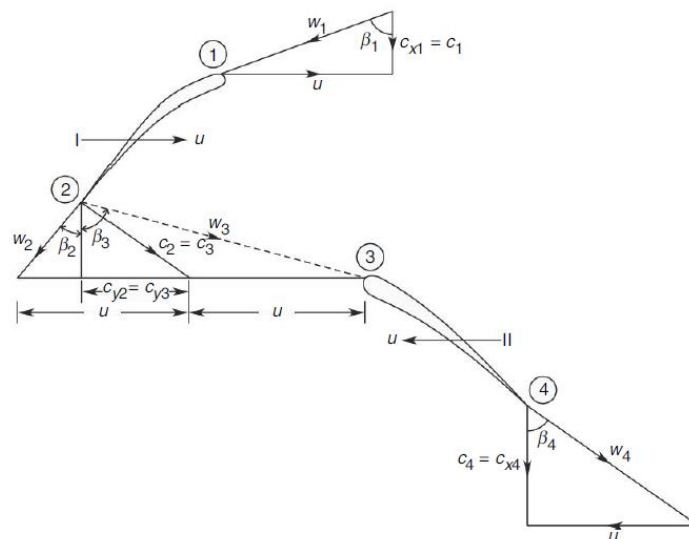
Figure 3.20 Velocity triangles of counter-rotating fan[29]

Since the air is directed axially in the first rotor, therefore the inlet swirling component is zero;

$$c_{y1} = 0$$

The absolute velocity exiting the first rotor is c_2 and the swirling component is c_{y2}, thus the work done associated with the first rotor is;[29]

$$w_I = u\left(c_{y2} - c_{y1}\right) = u\,c_{y2}$$

The velocity is received in absolute component and thus discharges it axially;

$$c_3 = c_2$$

$$c_{y4} = 0$$

$$c_{y3} = c_{y4}$$

The velocity triangles are drawn together for the inlet and outlet parts of the second ad first rotor respectively, the work done for the second rotor can be found by following expression;[29]

$$w_{II} = u\left\{0 - (-\,c_y)\right\}$$

$$w_{II} = u\,c_{y3} = u\,c_{y2}$$

Therefore, the total stage work comes out to be;

$$w_{st} = w_I + w_{II} = 2\,u\,c_{y2}$$

$$w_{st} = 2\,u\,(u - c_x \tan \beta_2)$$

$$w_{st} = 2\,u_2\,(1 - \phi\tan \beta_2)$$

The pressure rise can be expressed as;

$$\Delta p_{st} = 2\,r\,u_2\,(1 - \phi\tan \beta_2)$$

The pressure coefficient is;

$$\psi = 4\,(1 - \phi\tan \beta_2)$$

The static pressure rise for both the stages, the expression will be represented as;[29]

$$\Delta p_I = \frac{1}{2}\rho(w_1^2 - w_2^2)$$

$$\Delta p_I = \rho \, u \, c_{y2} - \frac{1}{2}\rho \, c_{y2}^2$$

$$\Delta p_{II} = \frac{1}{2}\rho(w_3^2 - w_4^2)$$

Since in the case under discussion, the geometry will be made using the rotor 1 as the inlet UGV,

$$\Delta p_{II} = \rho \, u \, c_{y2} - \frac{1}{2}\rho \, c_{y2}^2$$

$$\Delta p_{st} = 2 \, \rho \, u \, c_{y2}$$

3.6.3   Input Parameters

Following are the input parameters obtained after calculations,

Table 3-7 Input parameters of the 2-stage counter-rotating fan

Parameter	Value	Units
Thrust	88964	N
Diameter	1.27	M
Density	1.225	Kg/m^3
Pressure	101325	Pa
Coefficient of Pressure	1005	
Temperature	298	K
Gas Constant	287	
Area	1.2268	m^2

3.6.4   Performance Parameters

Following gives all the performance parameters of the lift fan system,

Table 3-8 Performance parameters of the 2-stage counter-rotating fan

Parameter	Blade 1	Blade 1	Blade 2	Blade 2 Outlet	Units
Beta	30.8	2.55	67.28	30.8	Degree
Absolute Velocity	204	131.82	204	131.82	m/s
Relative Velocity	237.51	-50.1	528.29	237.52	m/s
Pressure head	57485				m
Temperature	298		386.52		K
Enthalpy Change	88964				Joules
Mass flow rate	204				Kg/s
RPM	3068				
Pressure	101325		210310		Pa
Power	5178415.662				W
Density	1.225		1.896		Kg/m^3

3.6.5   Design Parameter Calculations

There are several design parameters which have to be considered for blade design process, these play an important role for the placement of the blade on the rotor with their angles incorporated, along with the inlet and outlet conditions being taken into considerations, following present the diagram of blade nomenclature in a cascade;
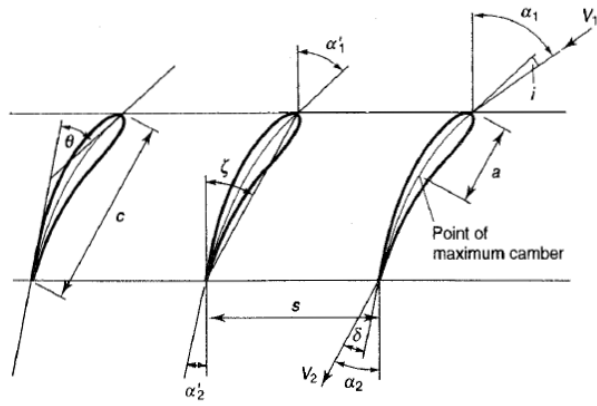
Figure 3.21 Blade Cascade[30]

The main parameters include the inlet and outlet angles of blade, air and velocity, along with angle of incidence, stagger angle, deviation angle, chord, pitch and deflection, each of these parameters play an important role in the blade configuration.[30] Stagger angle is between the reference plane and chord line of the blade, this mainly gives the orientation of the blade in accordance with the flow incoming which eventually affects the lift and drag properties. Pitch basically defines the blade spacing, and it can also be used to find out the number of blades on a rotor, it affects the pressure distribution and the flow across the cascade.[31] These parameters can be optimized for a better performance including thrust, efficiency and flow behaviors. [30]

The blade angles can be adjusted for an optimized model through the help of computational fluid dynamics for a high-performance blade design.[31]

3.6.6 Design Parameters

Following gives all the design parameters of the lift fan system,

Table 3-9 Design parameters of the 2-stage counter-rotating fan

Parameter	Stage 1	Stage 2	Units
Number of Blades	11	18	
Spacing	0.3593	0.1975	m
Stagger Angle	45	45	Degree

Solidity	0.6	1.1453	
Chord	0.1297	0.259	m
Mean Radius	0.5068	0.5068	m
Blade Length	0.2563	0.1612	m
Hub to Tip Ratio	0.5963		

3.7 Jowkousky Transformation for 0.6 Mach rotor

The blade geometry is dependent on the velocity triangles at inlet and outlet, but for that purpose the geometric parameters such as stagger angle, camber angle, camber line and thickness distribution are very important.[32] Preferably the blade geometry is adjusted according to the velocity triangles which is specific for a specific turbomachine, the blade design process itself is highly sophisticated, in order to achieve specific amount of efficiency, mass flow rates and other performance characteristics, it is necessary to follow the design process accordingly. The main process to generate the profile includes the generation of the camber line and the pressure and suction curves of the blade.[32]

A blade design mainly depends on the operating Mach number, for machines operating at 0.1 to 0.6 Mach number, NACA-65 profile series are considered more efficient, but for Mach number higher than the mentioned, Double circular arc (DCA) or the multi circular arc (MCA) profiles may be used. For high subsonic speeds the DCA and the MCA are used, even when DCA and NACA-65 series have the same pressure distributions but because of the sharp leading edges, the DCA profiles have high tip losses which eventually affects the efficiency of the machine.[32]

3.7.1 Bezier curve function

An interpolation tool used to generate straight lines, quadratic and cubic curves, with its vast applications in engineering in order to design any model which has the base of lines and curves, Bezier curve function serves the role. For the blade design process, a quadratic Bezier curve function is used, this function is represented by following expression, [33]

For x location,

$$B_x(x) = (1 - x)^2 P_{0_x} + 2(1 - x) + x^2 P_{2_x}$$

For y location,

$$B_y(x) = (1 - x)^2 P_{0_y} + 2(1 - x) + x^2 P_{2_y}$$

The start of the curve is at P0 and the end is at P2, the tangent point in the blade profile generation is P1, these three points were used in order to generate the Bezier curve for the camber line in association with the blade properties of the inlet absolute angles.[33]

For P_0, P_1 and P_2,

$$P_{0_x} = 0$$

$$P_{0_y} = 0$$

$$P_{1_x} = \frac{1}{1 + \frac{\cot(\alpha_1)}{\cot(\alpha_2)}}$$

$$P_{1_y} = \frac{\cot(\alpha_1)}{1 + \frac{\cot(\alpha_1)}{\cot(\alpha_2)}}$$

$$P_{2_y} = 1$$

$$P_{2_y} = 0$$

These expressions and values when run through a code, they give a camber line in accordance with the inlet and outlet absolute angles as calculated in the velocity triangles.[32]

3.7.2   PS and SS curve

The pressure and suction sides are superimposed with the camber line which was generated from the Bezier curve function, along with the required thickness of the blade, the following figure shows the positioning of the pressure and suction sides along with the camber line.[32]
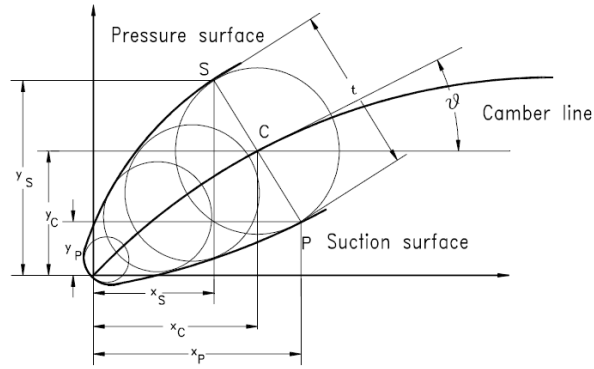
Figure 3.22 Multi Circular Blade Design[32]

Thus, for the generation of the pressure and suction sides, the following formulas were used for the x and y coordinates,

For θ,

$$\frac{dy(x)}{dx} = tg\theta = \frac{C_L^*}{4\pi} \ln \left(\frac{1 - \frac{x_c}{c}}{\frac{x_c}{c}} \right)$$
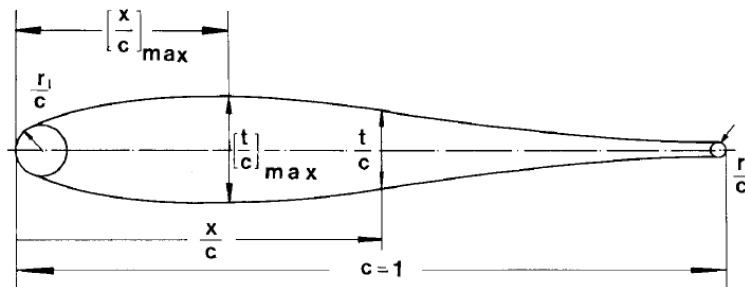

Figure 3.23 Blade Design Configuration[32]

For the pressure side and the suction side, the formulas used are,

Suction side,

$$x_{ss} = x_c - \left(\frac{t}{2}\right) \sin \theta$$

$$y_{ss} = y_c + \left(\frac{t}{2}\right) \cos \theta$$

Pressure side,

$$x_{ps} = x_c + \left(\frac{t}{2}\right) \sin \theta$$

$$y_{ps} = y_c - \left(\frac{t}{2}\right) \cos \theta$$

These relations are for the x and y coordinates of the pressure and suction sides of the blade profile, these are used in association with the camber line equations for the generation of the profile points of the blade curve.[32]

3.8   MATLAB code for modelling

Initially a code on MATLAB was written for the basic calculations of the design and performance parameters which were all the sets of equations which are mentioned in the design part of Chapter 3, these expressions were written in the code form since the velocity triangles include additional set of components for velocity and the angles, which are rotational, absolute and relative, also the total number of stage is 2, in which the total number of blades in one passage is 4, two for each stage of the counter-rotating fan. Therefore, to avoid complexity of solving these equations by hand, a MATLAB code was written while assigning similar notations for each variable.

3.8.1   Code for profile generation

All the expressions discussed related to the Bezier curve function, Pressure side, suction side, theta and the thickness of the blade, were written the form of a code in MATLAB. Thus, a profile of the all the variables were generated which was in the form of point data, these points were later on used in the generation of 2D and 3D CAD models which is discussed in the next section. Stage 1 profile for blades,
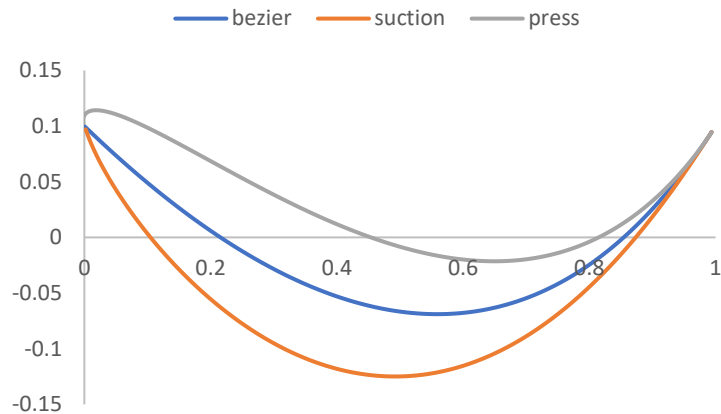
Figure 3.24 Blade 1 profile
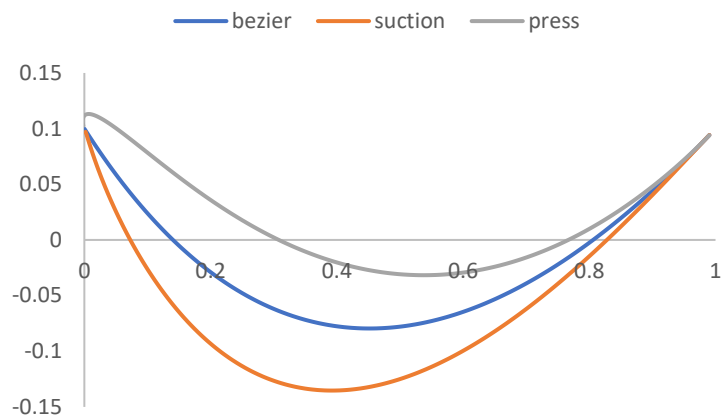
Stage 2 profile for blades,

Figure 3.25 Blade 2 profile

3.9   2-D to 3-D CAD Modelling

The profile points generated through the code had three lines, the camber line, suction side and the pressure side, therefore the main requirement was to generate a CAD model for the blade including only the suction side and the pressure side of the blade. The CAD software used was ANSYS Design Modeler to import the profile points and then to make a 3-D model from it.

3.9.1   CAD Modelling in ANSYS Design Modeler

ANSYS Design modeler is a CAD software for designing geometries, but it specifically can be used to generate CAD models for rotating machines, such as rotors of axial, radial, mixed flow

turbomachinery, even for diffusers, fans. These geometries are easy to import for meshing in ANSYS TurboGrid for high quality structured meshing.

The main procedure of the modeling in ANSYS design modeler includes,

1. Importing of profile points in a specific format in x, y and z format. The points have to be written in text file which can be imported as a 3-D curve. The profile curves of the x and y coordinates of pressure side and the suction side of the blade airfoil are in separate files, which are imported separately in the same work file of the ANSYS blade modeler.
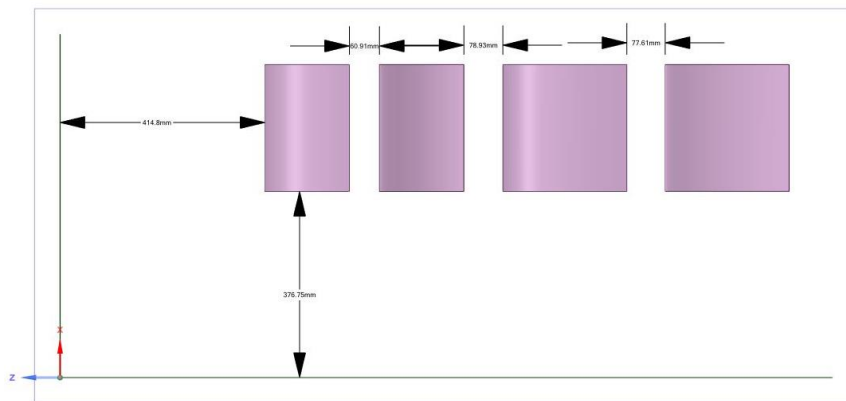

Figure 3.26 Blade positioning of counter-rotating fan

2. Then the blade is oriented according to its position in rotor, while keeping Z as the rotational axis, the length of the blade is kept according to the size by adjusting the scaling, and the angle of incidence and the position is set according to the calculations made in the design process.
3. Next the sketches of the hub, shroud, inlet and outlet of the blade passage is made in the ZY axis, only one blade passage is required for meshing and CFX simulations for CFD. Therefore, the sketch has to be made according to the position and the length of inlet and outlet.
4. Then using the flow path tool, the named boundaries of hub, shroud, inlet and outlet were assigned along with the 3-D blade, the flow path lines were made from the inlet to the outlet while capturing the blade profile.
5. Rotor spacing is a key integral while designing a counter-rotating fan, the space was kept at about 20% of the chord length of the blade in each stage of the lifting fan.[34]

6. The flow path profile of the blade passage was then exported as points and curve files, which was then to be imported in the ANSYS TurboGrid for meshing.
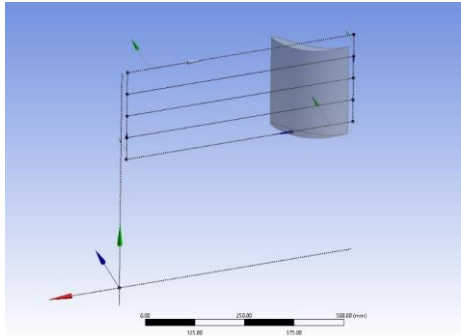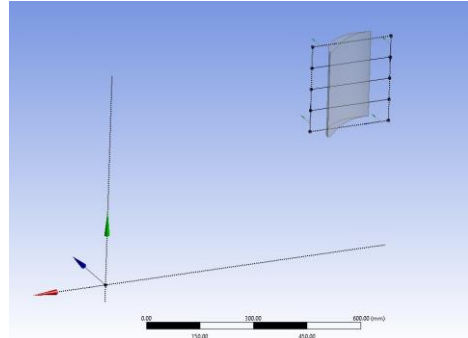

Figure 3.27 Flow path of Blade 1

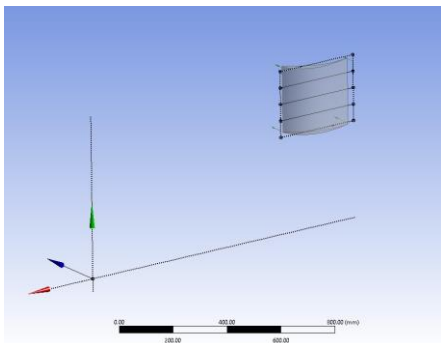**Figure 3.28** Flow path of Blade 2
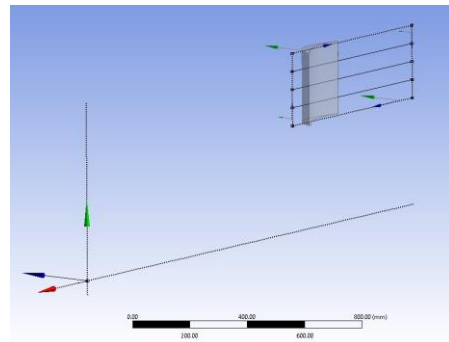

Figure 3.29 Flow path of Blade 3

Figure 3.30 Flow path of Blade 4

7. This process was repeated for the next three blade sets of the two-stage fan containing 4 rotor sets. All of these profile points and curves were imported in ANSYS TurboGrid.

3.10 TurboGrid meshing

ANSYS TurboGrid is a high accuracy ANSYS module which is used for meshing of turbomachinery components, it captures the blade profiles along with the passage details, as periodic boundary conditions, it provides with high quality meshes capable of capturing complex, leading and trailing edge profiles, it improves the mesh quality while minimizing the skewness while increasing the orthogonal quality since the mesh generated is structured. The

interfaces among the blade passages are also assigned that is for each blade row, which helps in presenting the results in a much accurate manner.

Following shows the mesh topology of the passages with the requirement of $Y^+ = 1$
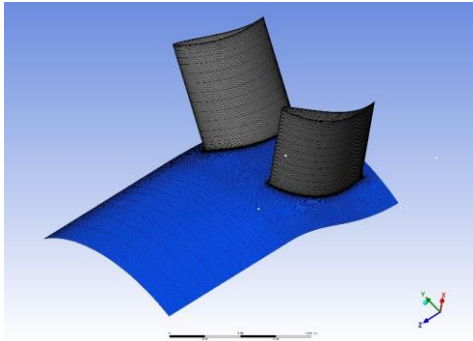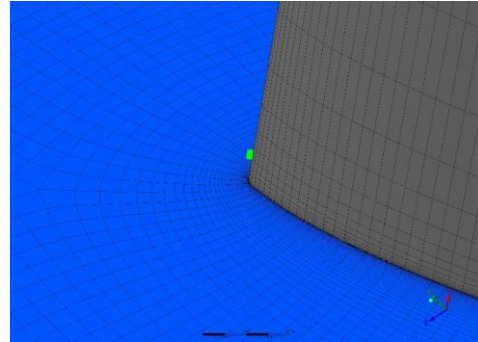

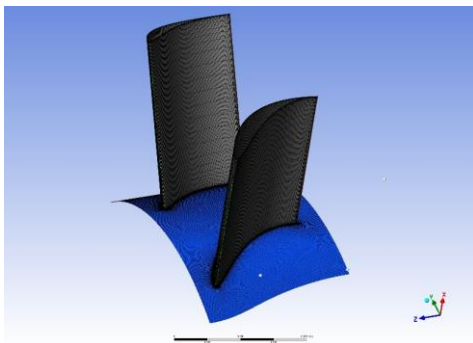**Figure 3.31** Mesh on rotor 1

Figure 3.32 Zoomed Mesh on rotor 1
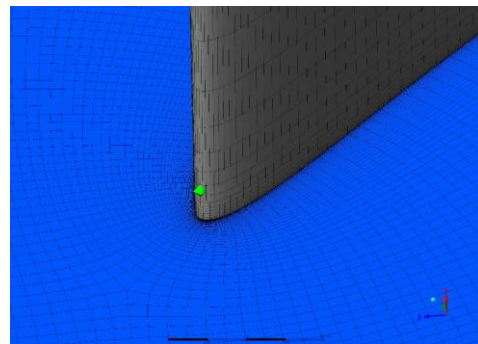

Figure 3.33 Mesh on rotor 2

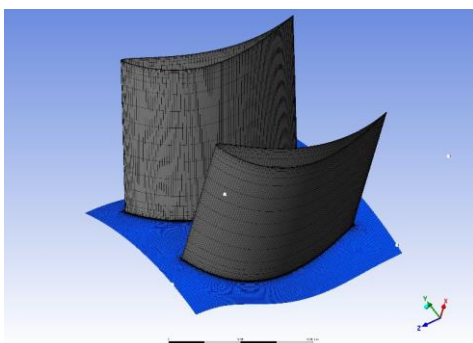
Figure 3.34 Zoomed Mesh on rotor 2

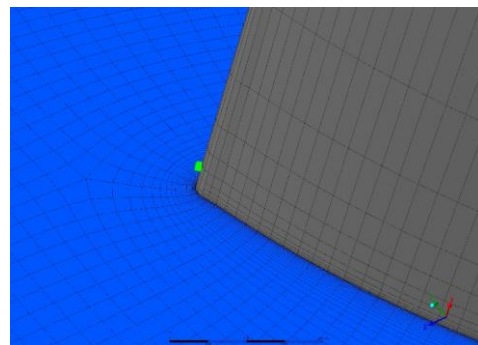**Figure 3.35** Mesh on rotor 3

Figure 3.36 Zoomed Mesh on rotor 3
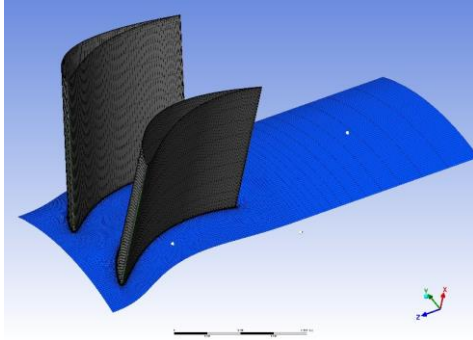
Figure 3.37 Mesh on rotor 4
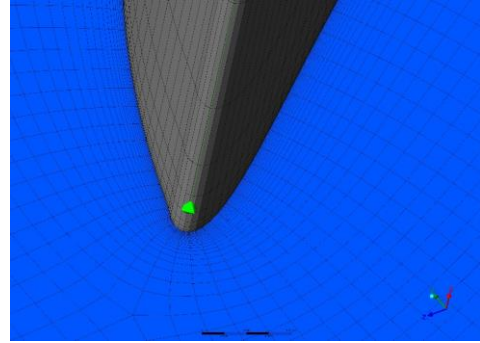
Figure 3.38 Zoomed Mesh on rotor 4

3.10.1 Blade Profile Meshing

Since the blade profile is exported in the form of curves and points, therefore these are then imported in ANSYS TurboGrid, which automatically makes the CAD profile using these profile curves and points. The initial mesh settings were made in a manner in order to capture the leading edge, trailing edge, and the blade tip. The boundary layer profile was also defined for Reynold's number 2820498.5 at 0.6 operating Mach number and at sea level boundary conditions.

Following shows the number of elements and nodes in each blade passage.

Table 3-10 Mesh information of the 2-stage counter-rotating fan

Blade Number	Number of Nodes	Number of Elements
Blade Passage 1	576480	550797
Blade Passage 2	729675	699864
Blade Passage 3	247349	232020
Blade Passage 4	181764	169026
Total	1735268	1651707

3.11 CFX Simulation for counter-rotating fan

In order to simulate a two-stage counter-rotating fan, ANSYS CFX provides a detailed CFD approach to calculate the performance parameters efficiently. Initially the CAD model designed as mentioned in the previous topics, is imported in the CFX module of ANSYS, CFX is a high-fidelity tool to compute the CFD results of turbomachinery components, initially the appropriate boundary conditions are set for the inlet and outlet in order to find out the results.

3.11.1 CFD setup

The flow path lines and the blade profile curves and points imported in ANSYS TurboGrid were used for structured meshing, the mesh was performed on the four blade sets which were imported in one CFX module. Different cases were run for various pressure outlets varying from 0atm to 2atm, this provided with the variation of inlet and outlet pressures and the mass flow rate variation which is an integral part in finding out the thrust of the system.

Since the boundaries were defined in the ANSYS Blade Modeler, which was then implemented in the ANSYS TurboGrid. The inlet, outlet, interfaces, periodic boundaries and the mixing planes were assigned between the blade passages, each blade passage was numbered according to their positioning defined in the CAD modelling process.

The rotational speeds were assigned to all the blade sets, the operating RPM was 3000, but the simulations were conducted at various RPMs in order to find out a better design point for the accurate mass flow rate and thrust, therefore the wall boundary conditions were are also implemented at the hub, shroud and the blades to ensure accurate CAD model for the CFD simulation process.

3.11.2 Boundary conditions

As boundary conditions play an important role in the CFD simulation, therefore appropriate boundary conditions were applied. Following shows the conditions applied at the boundaries and the solver models used,

Table 3-11 Boundary conditions of the 2-stage counter-rotating fan

Conditions	Setup

Density	Air Ideal Gas
Reference Pressure	0 atm
Pressure Inlet	1 atm
Pressure Outlet	0 atm – 2 atm
Turbulence Model	SST K-ω
Temperature Inlet	298 K
Interfaces	Stage Mixing Plane
Hub, Shroud, Blade	Wall Boundaries
Passage Sides	Periodic Boundaries
Heat Transfer Model	Total Energy
Axis Definition	Coordinate Axis
Domain Motion	Rotating
Buoyancy Model	Non-Buoyant

4 RESULTS AND DISCUSSION

The experimental study for the cruise condition of the aircraft, vertical take-off and landing, and the experimental study of the 2-stage counter-rotating fan is a much challenging task, therefore to overcome these hinderances, CFD simulations are performed in order to visualize and validate the flow physics, performance and efficiency of all of these systems. This milestone was achieved using the ANSYS Fluent and ANSYS CFX respectively. These are high fidelity tools for the computational fluid dynamics of such systems as mentioned above.

Usually, the CFD of the cruise condition of an aircraft is performed to optimize the geometric model of the aircraft or to find out the performance of specific components, but in the case mentioned, the geometry of the aircraft was not exact since the CAD model of F-35 is highly qualified. As discussed in the CAD section of the cruise validation, it is mentioned that the height, wing span and the fuselage size were kept according to that of the F-35 along with the geometric similarity, in order to visually validate the behavior of the flow physics in the transonic condition from zero to five degrees of angle of attack, the velocity magnitude contours were observed to view the formation of high velocity regions at the given conditions.

For the VTOL case, the simulation was performed in ANSYS Fluent, the main purpose of this simulation was to observe the behavior of the fluid flow when the aircraft is in cruise mode, this provides with a deep insight of the working of dynamic meshing using the overset conditions, which was done using the velocity inlet conditions at the fan outlet, nozzle outlet and the roll posts. Again, there was not sufficient data to validate the process, therefore the visual validation was performed for observing the flow physics of the Next Generation Fighter Aircraft (NGFA) in Vertical Take-off mode.

Finally, after the extensive design and modelling of the 2-Stage Counter-rotating fan, the CFD simulations were performed, the main purpose of the simulation was to acquire a lift fan which has the capability to provide 80KN of thrust,[11] which was much suitable for the lift-off of the NGFA having VTOL capabilities. Along with this, another important parameter, mass flow rate, was also observed in comparison to the pressure ratio at various pressure outlet conditions. Along with these factors, several other factors were also considered, which included, isentropic efficiency, swirling motion at inlet and outlet, pressure and velocity variation along the

rotational axis in all the rotors, thrust comparison at various RPMs apart from the design RPM, in order to find out the difference in behaviors of the fan at different power input conditions

The cruise validation was performed in order to find out the flow physics suitable for the aircraft which can perform various tasks within one aircraft, such as cruise, dog fight, fly at high Mach numbers, perform maneuverable tasks, take-off and land vertically just like a hovercraft. This provided with suitable results for the aircraft which would be suitable for the VTOL mode as well, after finding out the behavior of the flow physics in the cruise case, it was found out that the model may be suitable for VTOL conditions as well, therefore the boundary conditions applied to the system were according to that if the thrust surfaces in the VTOL CFD simulation. Therefore, in order to find the implementation of the VTOL results, a Lift fan system had to be designed, thus the extensive process of blade design, CAD modelling, meshing and CFD simulations were performed to find out a suitable lifting fan which may have the capability to provide 80KN of thrust, but after finding out the results, it came to light that there were more design considerations which had to be considered in order to design a lifting fan which may provide thrust equal to or more than the design requirement.

4.1   Cruise results

It is important to visualize the CFD results of an aircraft in order to find out the behavior at various angle of attacks and various Mach numbers, to visualize the flow behavior, which is mainly done through, streamlines, path-lines, contours and animations. The main purpose is to visualize the swirling motion of the air, the downwash effects, the high- and low-pressure field, high and low velocity regions, these identify the lifting surfaces along with the surfaces which contribute to form drag and induced drag, which force the aircraft into the stalling region after achieving the maximum coefficient of lift, following show various behaviors of the contours which tell about the parameters discussed above.[18]
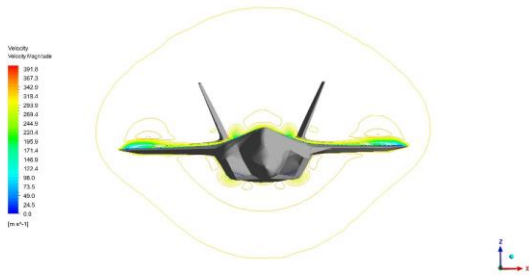
Figure 4.1 The velocity contours in the XZ plane shown at the trailing edge of the wing, shows the formation of wake and high velocity regions
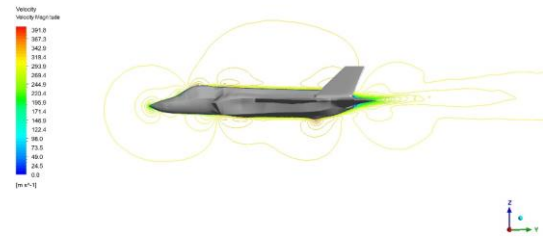
Figure 4.2 The velocity contours in the YZ plane shown at the mid-section of the fuselage, shows the high and low velocity along with stagnation points
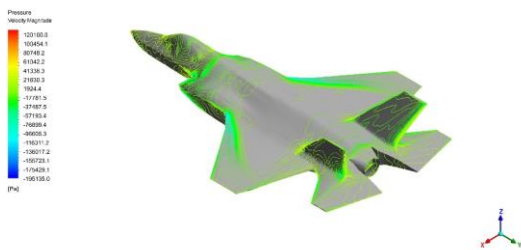

Figure 4.3 Static pressure contours, showing high- and low-pressure regions from the back of the aircraft highlighting the trailing edges
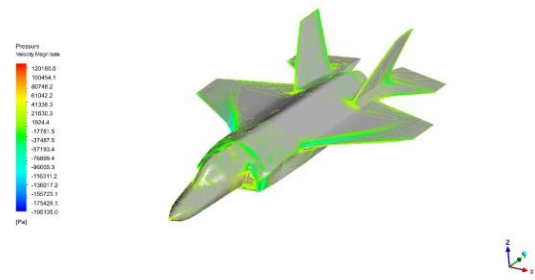
Figure 4.4 Static pressure contours, showing high- and low-pressure regions from the back of the aircraft highlighting the air intake and the leading edges
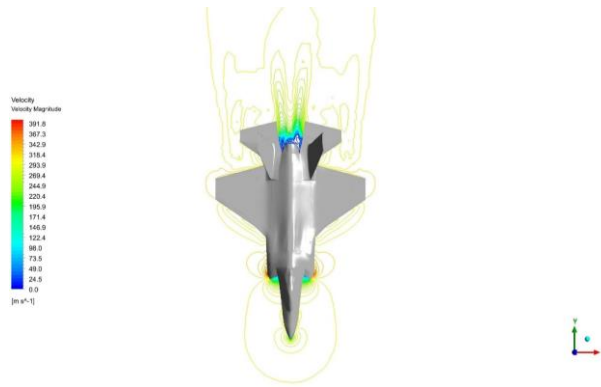
Figure 4.5 The velocity contours in the XY plane shown at the mid surface of the aircraft, shows the formation of wake at the aft surfaces of wing and tail, along with high velocity regions and stagnation points.
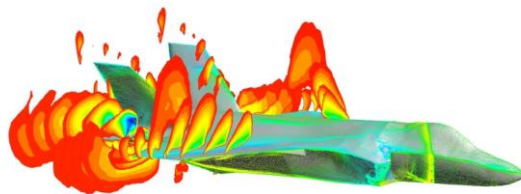

Figure 4.6 The velocity contours in the ZX plane shown at the trailing edge of the wing, shows the formation of wake on the wing and high velocity regions, this shows the results at a very high angle of attack

4.2   VTOL Results Discussion

The overset VTOL simulation provided with deep insights regarding the behavior of the NGFA under VTOL conditions. The simulation performed was to observe the ground effects of the aircraft in VTOL mode. Initially the aircraft was at rest on the ground with static boundaries, since the simulation was performed at unsteady conditions, which means that the time derivative in the Navier Stoke's Equations were taken into consideration while solving the CFD simulations. This provided with the visual effects of the aircraft from the zero-input velocity from, lifting fan, 3-BSM nozzle and the roll posts, and when the simulation progressed, the

flow started to develop at these specified locations, once the flow hit the ground, the ground effects started to play an important role in the reversal of flow towards the aircraft body, which provided a fountain like flow which created high pressure at the lower part of the aircraft. Thus, because of the trust positioning directed towards the ground and the pressure difference, the aircraft started to provide lift in the vertical direction which helped the aircraft to be lifted like a helicopter in straight vertical direction, since the weight of the aircraft was kept exact to that of F-35 B, the flow had to be developed sufficient enough which would be suitable to lift the aircraft while overcoming the weight of the aircraft.[18] In conventional aircraft take-off, an aircraft has four major forces in play, which help in take-off, lift, weight, drag and thrust, but in this case the major roles were played by only the lift from thrust and pressure difference and the weight which was countering the lift and thrust. Since lift and thrust were acting in upwards direction opposite to the weight, therefore it was suitable enough to lift the aircraft.

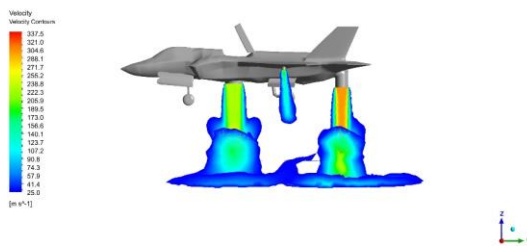Following shows the flow behaviors of the air flow in the VTOL mode through the help of CFD simulation results

Figure 4.7 Velocity magnitude at mid-section of the fuselage in YZ plane, showing the thrust flow from nozzle, lift fan and roll posts, showing the fountain formation in the middle
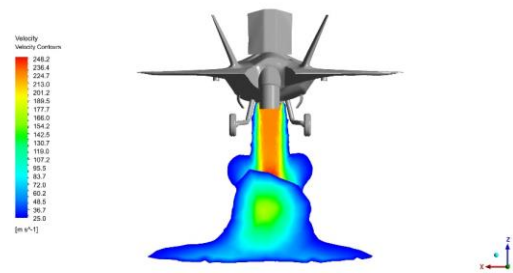
Figure 4.8 Velocity magnitude at mid-section of the Lift Fan in XZ plane, showing the thrust flow from lift fan and the ground effect due to it
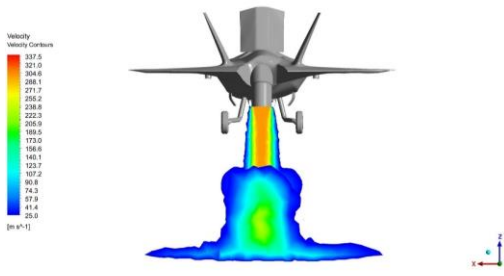
Figure 4.9 Velocity magnitude at mid-section of the nozzle in XZ plane, showing the thrust flow from nozzle and the ground effect due to it
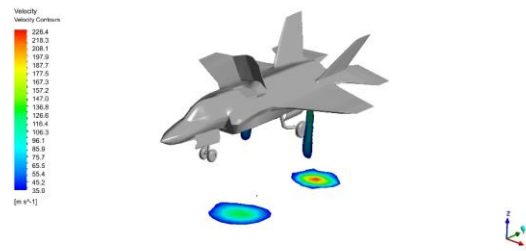
Figure 4.11 Velocity magnitude in the ISO plane, showing the velocity signatures on the ground due to the nozzle and the lift fan, showing the difference in the velocity
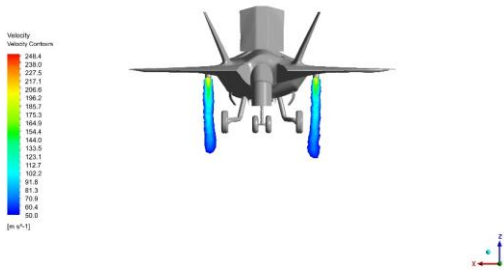

Figure 4.10 Velocity magnitude at mid-section of the roll posts in XZ plane, showing the thrust flow from lift fan, used for the rolling stability of the aircraft
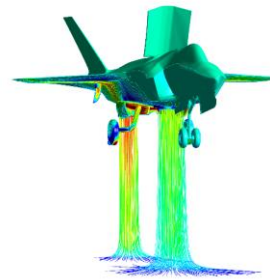
Figure 4.12 Velocity streamlines from the nozzle and the lift fan, along with pressure contours on the aircraft surface, it shows high pressure at the bottom for lift up

4.3 Ducted Fan Validation

The validation process was performed on the CFD simulation of the electric ducted fan, the results provided with the flow behavior of the velocity and pressure behavior at different blade spans of the rotor.[35] This provided with deep insights for the pressure ratio, volume flow rates and thrust of the ducted fan, the images below show a high pressure at the outlet of the ducted fan which is the major contributor of thrust by creating a pressure differential.

Figure 4.13 Pressure contours at 0.25 blade span, showing high pressure at outlet

Figure 4.14 Velocity contours at 0.25 blade span, showing low at outlet

Figure 4.15 Pressure contours at 0.5 blade span, showing high pressure at outlet

Figure 4.16 Velocity contours at 0.5 blade span, showing low velocity at outlet

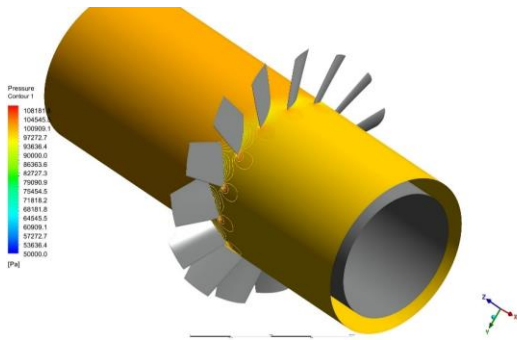**Figure 4.17** Pressure contours at 0.9 blade span, showing high pressure at outlet

Figure 4.18 Velocity contours at 0.9 blade span, showing low velocity at outlet
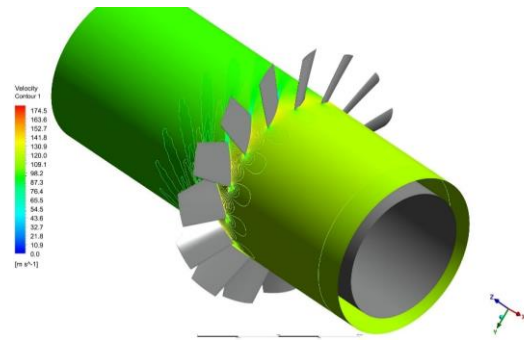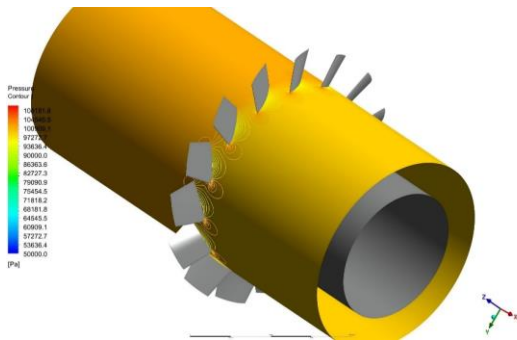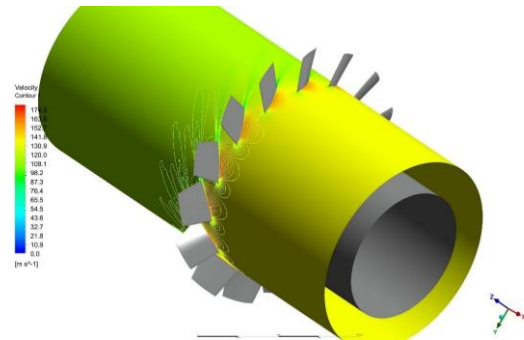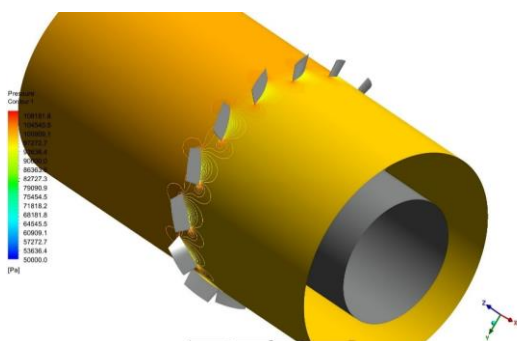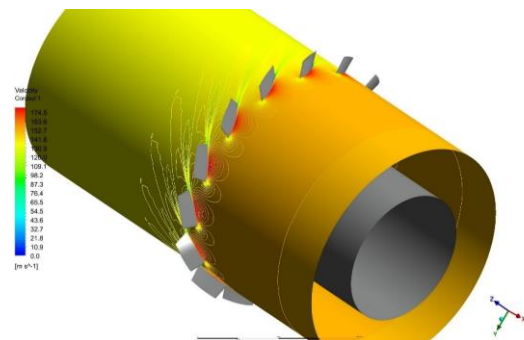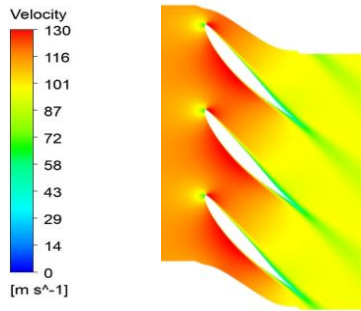
Figure 4.19 Velocity contours at 0.5 blade span, showing high pressure at outlet
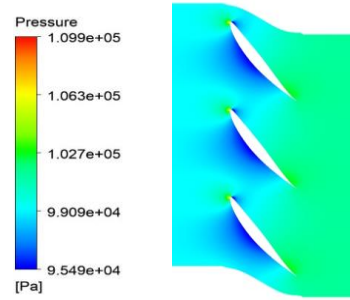
Figure 4.20 Pressure contours at 0.5 blade span, showing high pressure at outlet

After visualizing the flow pattern through the contours, it was important to observe the numerical results of the ducted fan, including the volume flow rate, the pressure rise and the thrust production, the CFD results show a very less error as compared to the experimental results of the original ducted fan model as shown below.

Table 4-1 CFD results of electric ducted fan

Sr.	Performance	Thesis	Validation	Units	Error
1	**Rotation Speed**	-2617.99	-2617.99	rad/s	-
2	**Reference**	0.0993	0.0993	m	-
3	**Volume Flow**	0.52114	0.5241	m^3/s	0.56
4	**Pressure rise**	2838.7	2952.13	Pa	3.99
5	**Thrust**	24.02629	25.04	N	4.2

4.4 2-Stage Counter-Rotating Fan Results

Finally discussing the results of the main part of the thesis, which is the two-stage counter-rotating fan. Since the flow in the rotor stages show a highly complex behavior, because in comparison to a compressor, where one stage contains a rotor and a stator, their combined flow physics is straightened because of the stator blades, but it is opposite in the case of a counter-rotating fan, since the first rotor directs air to the second one and the second rotor reduces the swirling effects and make the flow much streamline, which helps in the reduction of turbulent

losses, this also helps in increasing the efficiency of the system along with much suitable power input to avoid large amounts of power losses in order to rotate the impeller separately. The gear system used in these turbomachines are in coordination which helps in reducing the input power requirement unlike the conventional compressors or fans. This also helps in the reduction of swirl losses since the counter-rotating factor reduces the swirling effect and therefore it helps reducing the vortex formation.

Another important factor while observing the flow physics is the distribution of pressure around the stages, because this pressure differential helps in the production of thrust in fans, especially in the case of counter-rotating fans. Since while designing the blade, a few design considerations were ignored in order to avoid complexities, these included the hub design, blade twist, blade length variation, due to these factors the pressure gradients somewhat provided adverse effects which resulted in a decrease in efficiency, therefore these factors have to be monitored and corrected in the future versions of this design.[36] Due to this reason, a very high velocity was observed at the blade tips, but later on in the optimized models, it is suggested to study the tip clearance effects as it also effects the efficiency of the turbomachinery. Since these adverse pressure gradients produce swirling along the blade length due to the absence of the blade twist, this results in generation of vibrations as well which may result in damaging of the rotors as well, therefore the operational range of the rotational velocity of both the stages were kept the same.[37]

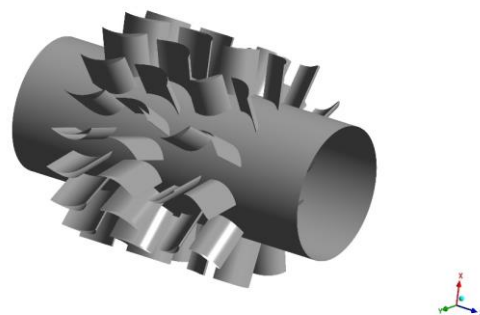Following shows the complete CAD model of the 2-Stage counter-rotating fan.

Figure 4.21 Full scale CAD model of the 2-Stage Lift fan system with hidden shroud for better visuals

4.4.1 CFD Results

The two major contributors while viewing the contours of the CFD simulations are velocity and pressure, their difference provide with much data that can be used to deduce much information about the flow behaviors, swirling, pressure ratios, flow rates, turbulent regions, shockwave formation, high temperature regions and several other factors as well. Some of these factors are discussed in the following images.

Figure 4.22 Pressure contours at 0.25 blade span, showing high pressure at outlet, with a pressure ratio of 1.8

Figure 4.23 Velocity contours at 0.25 blade span, showing low velocity at outlet, at around 0.6 to 0.9 Mach
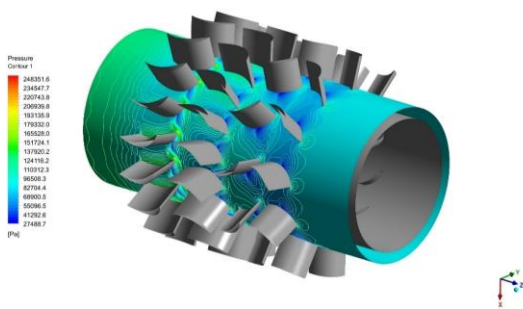

Figure 4.24 Pressure contours at 0.5 blade span, showing high pressure at outlet, with a pressure ratio of 1.8
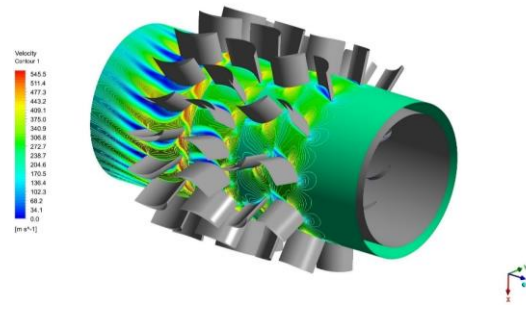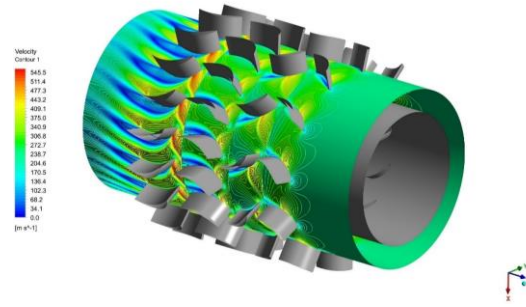

Figure 4.25 Velocity contours at 0.5 blade span, showing low velocity at outlet, at around 0.6 to 0.9 Mach
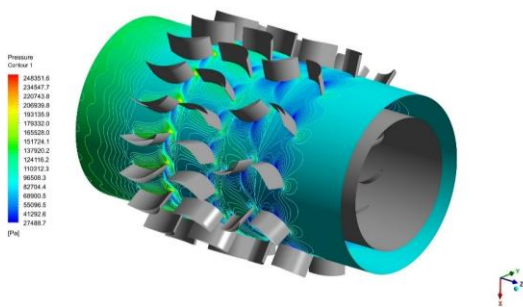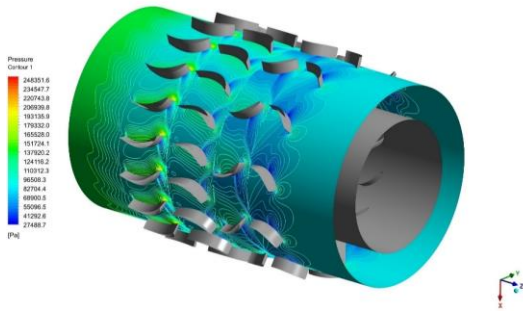
Figure 4.26 Pressure contours at 0.75 blade span, showing high pressure at outlet at around 1.7 atm
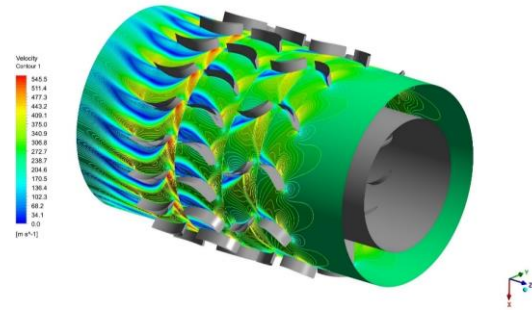
Figure 4.27 Velocity contours at 0.75 blade span, showing low velocity at outlet, at around 0.8 to 0.9 Mach

Mainly at high blade span, the velocity increases due to tip losses and high moment arm of the blade from the hub of the impeller, which increases the velocity at the trailing edge span wise and at the blade tip.[38] In order to observe the effects of velocity, the main high velocity regions are created due to the stagnation points, where the flow directly hits and stops suddenly, this creates high pressure regions and high velocity regions as well, since the flow moves towards choking, as it can be seen that these effects are reduced due to the rotation of rotors in the upcoming passages.
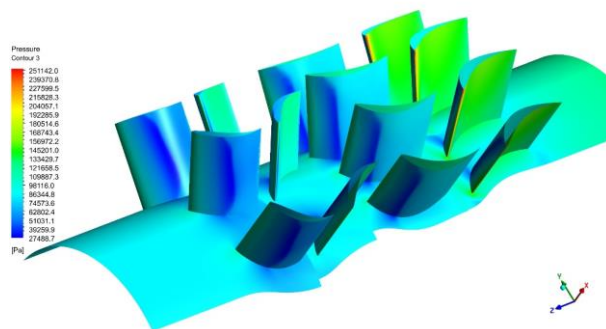
Figure 4.28 Static pressure contours along the fan, from inlet to outlet, with an increased pressure at the outlet which helps in the production of thrust

The pressure side and the suction sides are mentioned clearly which can be visualized through the pressure contours, the pressure at outlet ranges from 1.7 to 1.9 atm, which is the main contributor in the production of thrust.
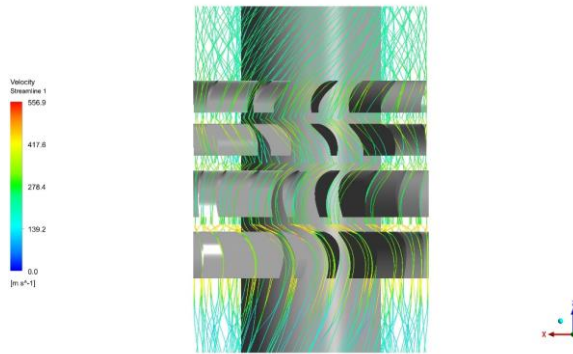
Figure 4.29 Velocity streamlines, inlet is at the top and outlet is at the bottom, this shows a clear reduction un the swirling effects due to the counter rotation of the rotors

It is important to view the effects of pressure and velocity at the rotor passage interfaces, or the faces in between two rotors.[39] The pressure at each face is increasing as moved from one rotor to the other. These show the gradual increase of pressure at each rotor exit which is an important parameter to consider, since the flow reversal because of any rotor can cause surging and can prove to be catastrophic for the turbomachinery if not noticed and solved timely.
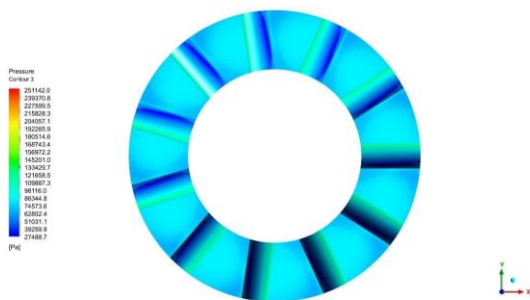
Figure 4.30 Pressure contour at interface between blade 1 and 2
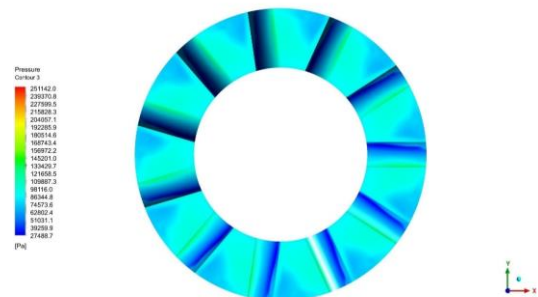
Figure 4.31 Pressure contour at interface between blade 2 and 3, showing a gradual increase in pressure
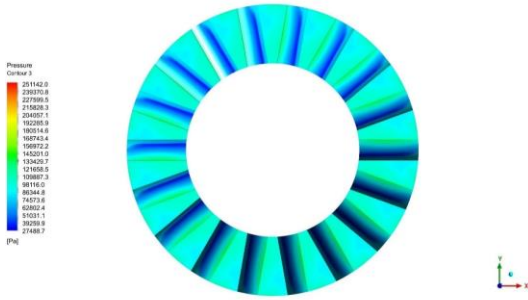
Figure 4.32 Pressure contour at interface between blade 3 and 4, showing a gradual increase in pressure
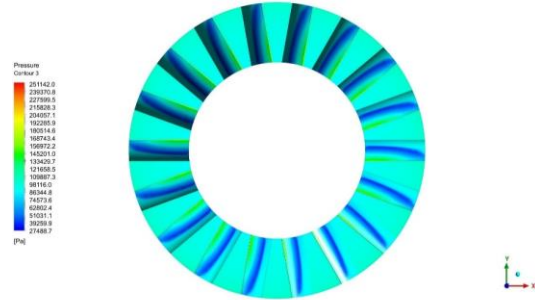
Figure 4.33 Pressure contour at interface at exit of blade 4, the pressure is much higher as compared to the previous interfaces

After the visualization of pressure variations, it is important to view the blade-to-blade contours to understand the flow physics in a better way, thus to view the flow physics, the blade-to-blade view is seen at different spans of the blade.
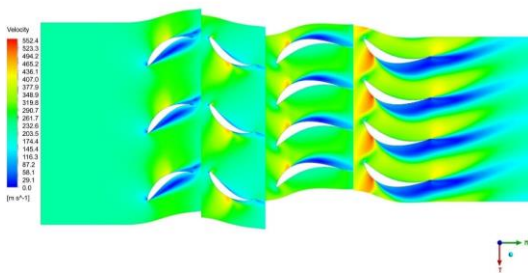
Figure 4.34 Velocity contour at 0.25 span of the blade
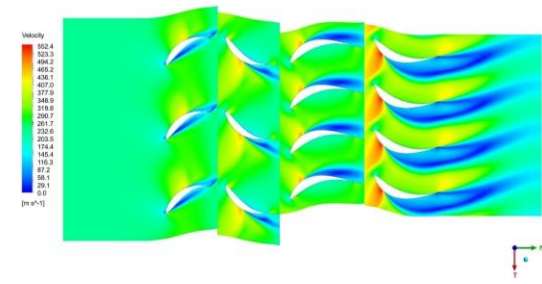
Figure 4.35 Velocity contour at 0.5 span of the blade

As moved from low blade spans to higher, it can be clearly seen that there is an abrupt increase in the velocity at the leading edge of the rotor 2 of the stage 2, this is due to the absence of the blade twist and the constant span of the blade, since in general trends the chord length of the blades are smaller than that at the root of the blade, this helps in reduction of tip losses and swirling in the blade, which causes turbulent losses at the blade throughout the span due to circulation from pressure side to suction side.
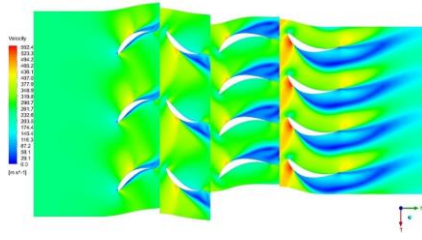
Figure 4.36 Velocity contour at 0.75 span of the blade
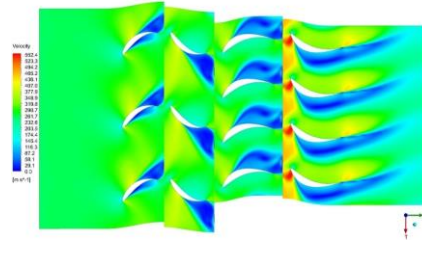
Figure 4.37 Velocity contour at 0.9 span of the blade

4.4.2 Characteristic Curves

One of the most important performance graphs is the characteristic curve in a turbomachinery component, since this gives a detailed view of the variation of pressure ratio at various flow rates. To observe the trends in this graph, it is important to operate the machine at various RPMs in percentage of the design RPM. In this lift fan case, the design RPM was kept at 3000, and for simplicity, all the rotors were kept at the same RPM, and their directions were according to the blade orientation. RPMs ranging from, 2500, 3000, 3500, 4000, 4500 and 5000 were simulated at various pressure outlet conditions with an increment of 0.1atm, this provided with the visualization of the increase in pressure ratio at the outlets, which gave various pressure ratios, in order to find the design point of the machine. The maximum mass flow rate was obtained, which is 153.876kg/s, at 5000 RPM, and this was used to normalize all the other mass flow rates at other RPMs to observe the general trend in all the RPM ranges.
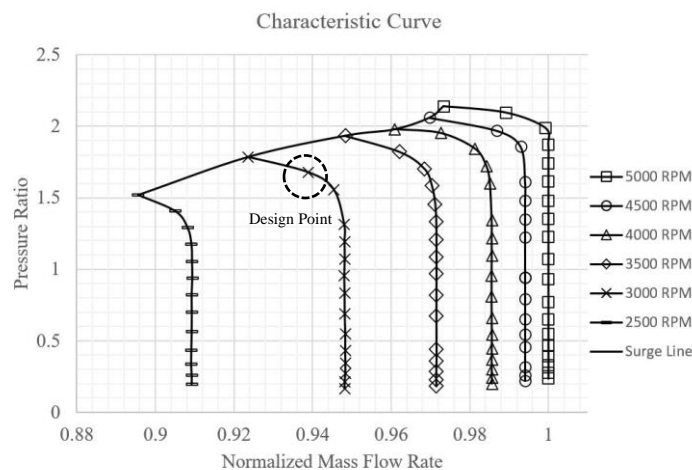
Figure 4.38 Characteristic curve shows the CFD results mentioning the pressure ratios and mass flow rates at various RPM ranges

After a certain pressure outlet range, the mass flow rate starts to decrease gradually and after achieving the choking condition, the flow stops and that is represented by the surge line. This provides with the limitation of the turbomachinery at specified pressure ratio. The design point is mentioned in the graphical representation, at which the lift fan was designed.

4.4.3 Efficiency discussion

The efficiency plot was made separately for each RPM in order to find out, if the lift fan would be efficient at any other RPM or not, but it can be clearly seen in the trend that the maximum efficiency was acquired at the design ROM only, and the rest of the RPMs show a huge decrement in the isentropic efficiency.
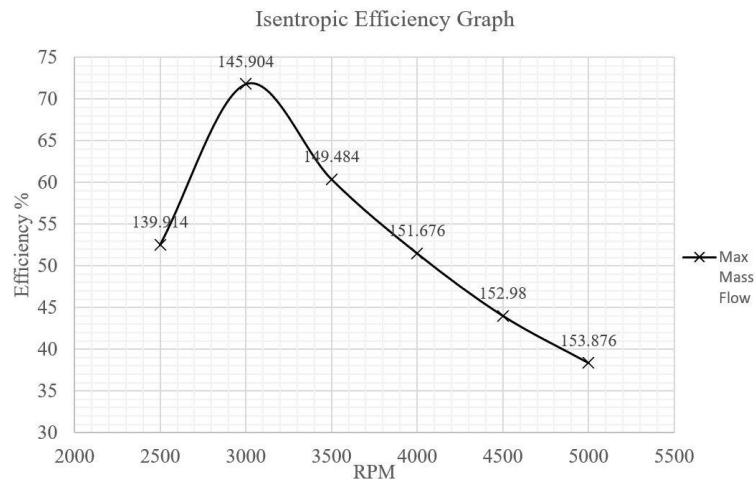
Figure 4.39 Isentropic efficiency graph, showing the mass flow rate values at the specified RPMs

This is due to the increase in the input requirement as compared to that of the design requirement of the lift fan which diverts from the limitation of the machine, but these simulations had to be performed to find out the choking, surging, maximum efficiency.

4.4.4 Swirling effects

One of the major advantages of a counter-rotating fan is that it reduces the swirling effects, as discussed earlier, swirling can cause turbulent losses, which causes a major decrease in the performance of the turbomachinery,[40] it causes vortex losses along with swirl losses which is caused mainly by circulation of flow, this the induces surging which limits the turbomachinery to produce less amounts of thrust.
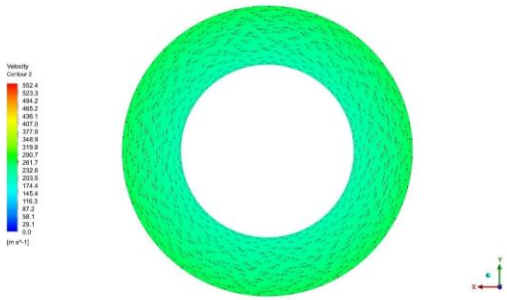
Figure 4.40 Velocity contour at inlet face, with high swirling motion of the velocity components
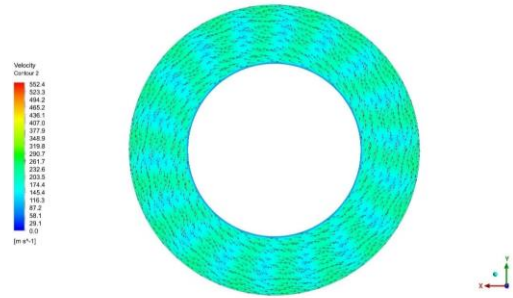
Figure 4.41 Velocity contour at outlet face, with less swirling motion of the velocity components

Another important way to visualize the swirling effects is to view the velocity contours at the blade interfaces, this shows the gradual reduction in the swirling effects as the counter-rotating phenomenon helps in reduction of the swirling effect.[41] Following shows the velocity contours at each rotor exit.
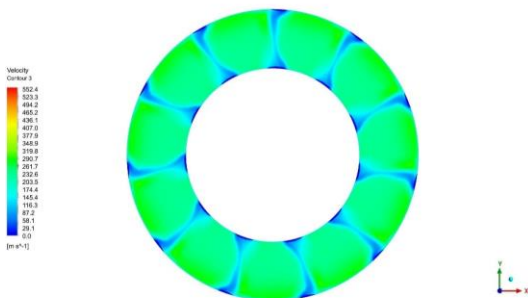
Figure 4.42 Velocity contour at interface between blade 1 and 2, swirling is observed through the flow motion
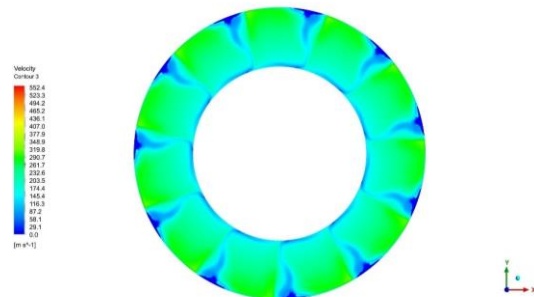
Figure 4.43 Velocity contour at interface between blade 2 and 3
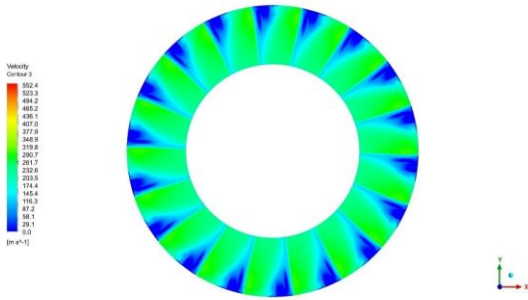
Figure 4.44 Velocity contour at interface between blade 3 and 4, swirl reduction
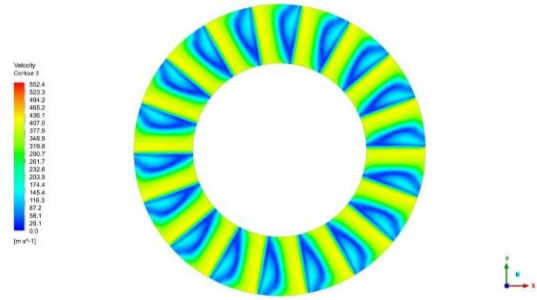
Figure 4.45 Velocity contour at the exit of rotor 4, this helps in reducing the swirling effects and helps in directing the flow

4.4.5 Density and Pressure Head

While discussing these parameters, it is important to observe the density changes along with the change in Mach number, since at high subsonic and at transonic flow regimes, the flow becomes compressible and the compressibility effects start playing a major role in changing the flow physics. Thus, density is the major factor which changes with the change in Mach number. The results shown in the graph below are the representation of density with respect to Mach number, both at outlet face, due to very low pressure at outlet, the flow tends to reach at high Mach numbers, but those results are not realistic, since these low pressures are not operational in experimental phase, therefore the operating range is mentioned in the graph below.
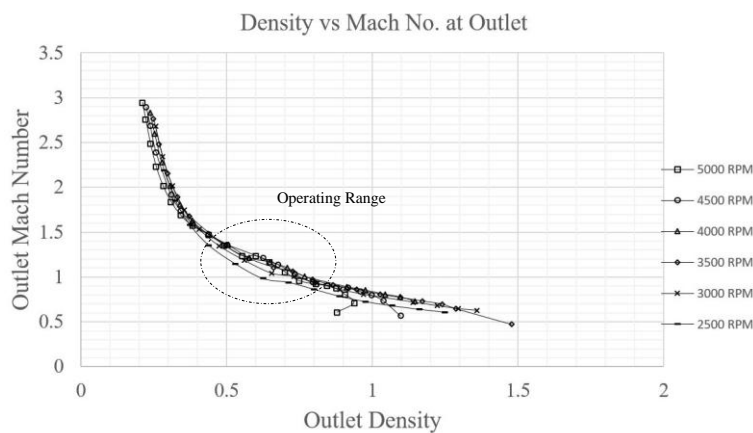
Figure 4.46 Variation of density with respect to Mach number at varying RPM ranges

The pressure head at inlet was also compared with normalized mass flow rates, each line in the trend shows the variation of inlet pressure head with respect to their operating RPM.
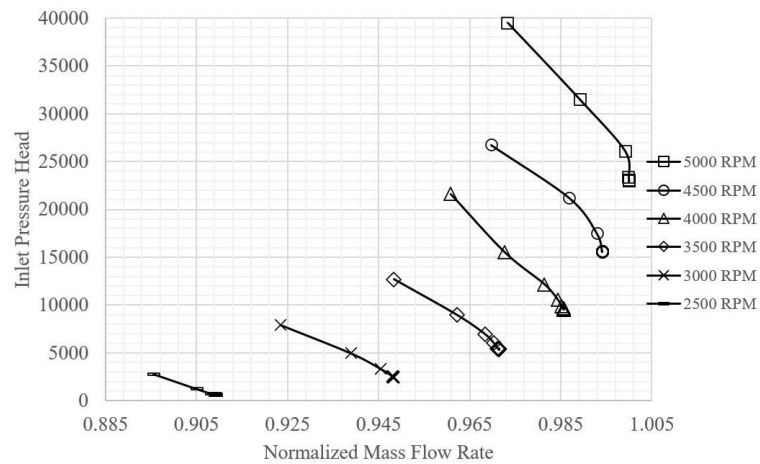
Figure 4.47 Pressure head at inlet vs the normalized mass flow rate

4.4.6 Thrust Analysis

Following shows the trends of thrust at varying pressure ratios, since the pressure ratios lesser than 1 are not suitable for the lift fan, therefore that region is mentioned as choking region, and pressure ratios greater than 1 provide with the actual required thrust, which is suitable for the performance of the lift fan.
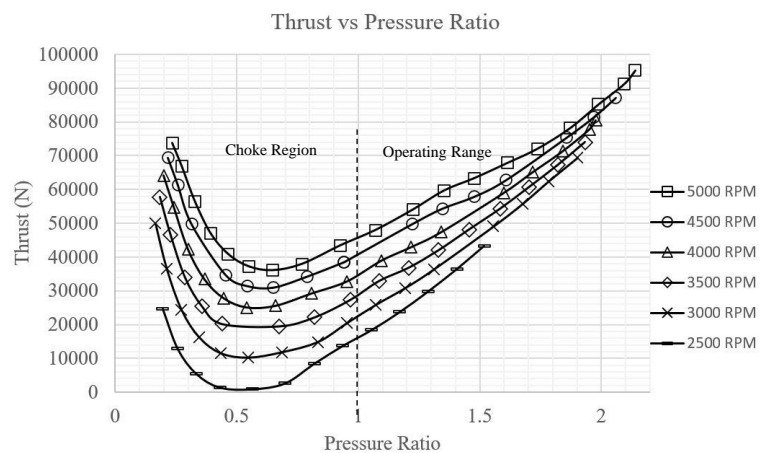
Figure 4.48 Thrust in comparison with pressure ratios for different RPMs

This following trend shows the thrust values at the specified RPMs, since the maximum thrust is produced at 5000 RPM, but it is not suitable since the efficiency of the lift fan is much lesser than the design RPM, which produced approximately 70KN of thrust at 3000 RPM.

$$T = \dot{m}_e v_e - \dot{m}_i v_i + (P_e - P_i)A_e$$

The thrust was calculated using the mass flow rates and velocity at inlet and exhaust, along with the pressure difference between inlet and outlet. Since the main goal of this thesis was to acquire thrust equivalent to 80KN, but due to several design limitations, this exact amount could not be achieved at the design point. The main function of a fan is to accelerate the out flow and this along with the pressure differential helps in the production of thrust, this can clearly be seen in the graph that the thrust is increasing with the increase in the pressure ratio, this can also be seen in the graph below as well since it clearly shows a linear trend in the increment of thrust with the increase in RPM.
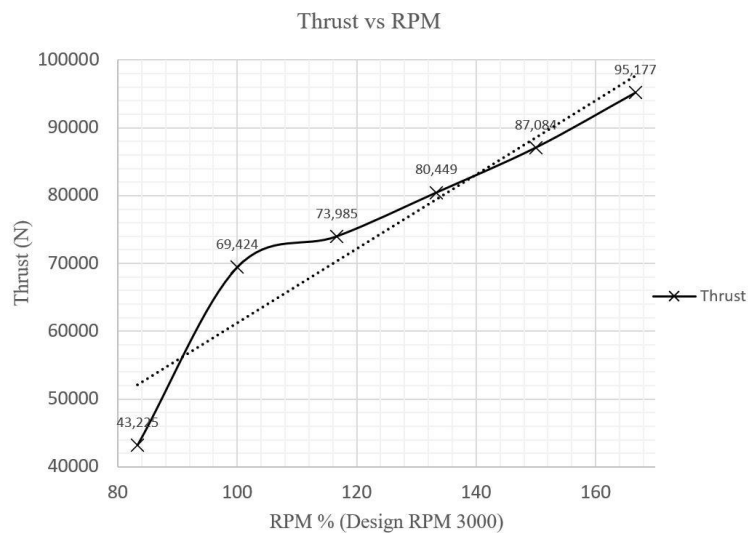
Figure 4.49 Thrust at various RPMs

This gives a total error of 12% in comparison to the 80KN of thrust, but it can be seen that with the increase in the RPM results in the increase of thrust, but it is not much suitable since it leads to the decrease in the efficiency of the turbomachinery as discussed in the previous sections.

5   CONCLUSIONS

This thesis is divided into three parts, the CFD of cruise of an NGFA, CFD of VTOL mode of an NGFA and the design and simulation of a 2-stage counter-rotating lift fan of an NGFA. The main connection between these three parts is to develop a framework which may support an NGFA into developing ability to hover like a helicopter, take-off and land vertically. Following are some of the key findings in this dissertation:

The flow physics over the surfaces of an NGFA are essential while considering the flow behavior in transonic regime i.e. cruise simulations. The VTOL mode is important to study the ground effects and thrust requirements for stable lifting of aircraft in straight upwards direction. Lift fan design process primarily depends on requirements identified from the VTOL simulations. Theoretical calculations utilized Bezier curves and Jowkousky Transformations to obtain blade profiles. The analysis suggested a two stage contra-rotating ducted fan with 50inch diameter designed to achieve 80kN thrust. To achieve 80KN thrust, pressure ratio of 1.9 at 3000 RPM and 204 kg/s mass flow rate was proposed.

To test the performance of the proposed lift fan, CAD model of a two stage contra-rotating fan was developed in ANSYS Design Modeler. ANSYS TurboGrid was utilized for meshing and the simulations were performed using ANSYS CFX. The simulation results showed an excellent agreement with the theoretical design calculations. The proposed two stage contra-rotating lift fan attained 71% efficiency to achieve the design requirements of 80KN thrust with 12% error. This process was then moved forward to the simulations gave a deep insight about the flow behavior and the performance parameters of the lift fan

The discrepancies in efficiency and thrust values observed during numerical simulations can be because of the design limitations. During design calculations some important features such as; blade twist, hub design and blade length in each stage are ignored.

In future work, it is suggested to fulfill these ignored design considerations and move towards an optimized model, specially of the blade, which is the only key contributor in the lift fan. These design considerations help in increasing the performance of the turbomachinery, mainly increasing the efficiency, which occurs because of the parameters discussed above, therefore it is highly suggested to design the blade accordingly. Also, the experimental testing of the lift fan will prove to be more beneficial since the CFD results are reliable to some extent, therefore

these considerations can be improved thoroughly if the design changes are made after the experimental testing of the manufactured product, but since it the design of a lift fan includes much more complexities other than just the blade design, it is much difficult to achieve the required machine.

6 REFERENCES

[1]   T. E. Ford, "Harrier II," Aug. 01, 1984. doi: 10.1108/eb036007.

[2]   I. A. Maddock and M. J. Hirschberg, "The quest for stable jet borne vertical lift: Astovl to F-35 stovl," in *AIAA Centennial of Naval Aviation Forum "100 Years of Achievement and Progress,"* 2011. doi: 10.2514/6.2011-6999.

[3]   P. M. Bevilaqua, "Genesis of the F-35 joint strike fighter," *J Aircr*, vol. 46, no. 6, pp. 1825–1836, 2009, doi: 10.2514/1.42903.

[4]   B. Atuk and A. Majchrowicz, "Dr. Paul bevilaqua: The brilliant mind behind the f-35b lightning ii," in *AIAA Scitech 2019 Forum*, American Institute of Aeronautics and Astronautics Inc, AIAA, 2019. doi: 10.2514/6.2019-0120.

[5]   A. Doddi, "Vertical Take-off and Landing (VTOL)," *American Institute of Aeronautics and Astronautics*, pp. 1–8, 2016.

[6]   Y. Zhou, H. Zhao, and Y. Liu, "An evaluative review of the VTOL technologies for unmanned and manned aerial vehicles," Jan. 01, 2020, *Elsevier B.V.* doi: 10.1016/j.comcom.2019.10.016.

[7]   P. Bevilaqua, "Inventing the F-35 joint strike fighter," in *47th AIAA aerospace sciences meeting including the new horizons forum and aerospace exposition*, 2009, p. 1650.

[8]   S. P. Wurth and M. S. Smith, "F-35 propulsion system integration, development, and verification," in *2018 Aviation Technology, Integration, and Operations Conference*, American Institute of Aeronautics and Astronautics Inc, AIAA, 2018. doi: 10.2514/6.2018-3517.

[9] D. G. Parsons, D. E. Levin, D. J. Panteny, P. N. Wilson, M. R. Rask, and B. L. Morris, "F-35 STOVL performance requirements verification," in *2018 Aviation Technology, Integration, and Operations Conference*, American Institute of Aeronautics and Astronautics Inc, AIAA, 2018. doi: 10.2514/6.2018-3681.

[10] D. Jensen and J. Leonard, "Rolls-Royce and Allison Lift Engines," in *43rd AIAA/ASME/SAE/ASEE Joint Propulsion Conference & Exhibit*, 2007, p. 5340.

[11] Rolls Royce, "VCOMB-4202-Rolls-Royce-LiftSystem-datasheet," 2023.

[12] Aerospace Technology, "F-35B Lightning II: VTOL Capabilities and the Two-Stage Counter-Rotating Fan," aerospace-technology.com. Accessed: Jul. 27, 2024. [Online]. Available: http://aerospace-technology.com/

[13] UAV Digest, "The Future of UAVs: VTOL Technology and Applications." Accessed: Jul. 27, 2024. [Online]. Available: uavdigest.com

[14] Defense Aviation, "VTOL Innovations in Modern Fighter Aircraft." Accessed: Jul. 27, 2024. [Online]. Available: http://defenseaviation.com/

[15] S. L. Karman and P. A. Wooden, "CFD Modeling of F-35 Using Hybrid Unstructured Meshes," 2009.

[16] P. M. Bevilaqua, "Joint Strike Fighter dual-cycle propulsion system," *J Propuls Power*, vol. 21, no. 5, pp. 778–783, 2005, doi: 10.2514/1.15228.

[17] D. Jensen and J. Leonard, "Rolls-Royce and Allison Lift Engines," in *43rd AIAA/ASME/SAE/ASEE Joint Propulsion Conference & Exhibit*, 2007, p. 5340.

[18] P. Wooden, B. Smith, and J. Azevedo, "CFD Predictions of Wing Pressure Distributions on the F-35 at Angles-of-Attack for Transonic Maneuvers," in *25th AIAA Applied Aerodynamics Conference*, 2007, p. 4433.

[19] I. Kuo, "The Incredible Versatility of the F-35 Lightning II," 2013.

[20] I. A. Maddock and M. J. Hirschberg, "The quest for stable jet borne vertical lift: Astovl to F-35 stovl," in *AIAA Centennial of Naval Aviation Forum "100 Years of Achievement and Progress,"* 2011. doi: 10.2514/6.2011-6999.

[21] X.-H. Yang and P. Shan, "Design of Two Kinds of Counter-Rotating Fans and CFD Investigation on Their Aerodynamic Characteristics," 2011. [Online]. Available: http://www.asme.org/abo

[22] T. Ebus, M. Dietz, and A. Hupfer, "Experimental and numerical studies on small contra-rotating electrical ducted fan engines," *CEAS Aeronaut J*, vol. 12, no. 3, pp. 559–571, Aug. 2021, doi: 10.1007/s13272-021-00517-7.

[23] P. Schimming, "Counter rotating fans—An aircraft propulsion for the future?," *Journal of Thermal Science*, vol. 12, pp. 97–103, 2003.

[24] A. F. Nemnem, M. Y. Zakaria, and A. M. Elzahaby, "Contra-rotating ducted fan aerothermodynamic design procedure for unmanned applications," in *AIAA Information Systems-AIAA Infotech at Aerospace, 2018*, American Institute of Aeronautics and Astronautics Inc, AIAA, 2018. doi: 10.2514/6.2018-0745.

[25] W. Y. Kim, S. Senguttuvan, and S. M. Kim, "Effect of rotor spacing and duct diffusion angle on the aerodynamic performances of a counter-rotating ducted fan in hover mode," *Processes*, vol. 8, no. 11, pp. 1–14, Nov. 2020, doi: 10.3390/pr8111338.

[26]   S. Deng and Z. Ren, "Experimental study of a ducted contra-rotating lift fan for vertical/short takeoff and landing unmanned aerial vehicle application," *Proc Inst Mech Eng G J Aerosp Eng*, vol. 232, no. 16, pp. 3108–3117, Dec. 2018, doi: 10.1177/0954410017731441.

[27]   J. Gertler, *F-35 joint strike fighter (jsf) program*, vol. 16. Congressional Research Service, 2012.

[28]   Y. Jiang and B. Zhang, "Numerical investigation of effect of parameters on hovering efficiency of an annular lift fan aircraft," *Aerospace*, vol. 3, no. 4, Dec. 2016, doi: 10.3390/aerospace3040035.

[29]   S. M. Yahya, *Turbines compressors and fans*. McGraw-Hill Education LLC, 2011.

[30]   S. L. Dixon, L. New York, and S. Diego, "Fluid Mechanics, Thermodynamics of Turbomachinery Fifth Edition, in SI/Metric units." [Online]. Available: www.semeng.ir

[31]   H. I. H. Saravanamuttoo, G. F. C. Rogers, and H. Cohen, *Gas turbine theory*. Pearson education, 2001.

[32]   Meinhard. Schobeiri, *Turbomachinery flow physics and dynamic performance*. Springer, 2005.

[33]   M. Abbas, E. Jamal, J. M. Ali, M. Abbas, E. Jamal, and J. M. Ali, "Bezier Curve Interpolation Constrained by a Line Mathematics Subject Classification: 68U05, 68U07, 65D05, 65D07, 65D18 1818," 2011.

[34]   W. Y. Kim, S. Senguttuvan, and S. M. Kim, "Effect of rotor spacing and duct diffusion angle on the aerodynamic performances of a counter-rotating ducted fan in hover mode," *Processes*, vol. 8, no. 11, pp. 1–14, Nov. 2020, doi: 10.3390/pr8111338.

[35] X.-H. Yang and P. Shan, "Design of Two Kinds of Counter-Rotating Fans and CFD Investigation on Their Aerodynamic Characteristics," 2011. [Online]. Available: http://www.asme.org/abo

[36] P. M. Bevilaqua, L. Martin, and S. Works, "Dual Cycle Operation of the Shaft Driven Lift Fan Propulsion System," 1997.

[37] J. E. Goebel, "Design of a lift fan engine for a heavy lift aircraft," Monterey, California. Naval Postgraduate School, 2003.

[38] J. G. Skifstad, "Aerodynamics of jets pertinent to VTOL aircraft," *J Aircr*, vol. 7, no. 3, pp. 193–204, 1970, doi: 10.2514/3.44146.

[39] Y. Jiang, B. Zhang, and T. Huang, "CFD study of an annular-ducted fan lift system for VTOL aircraft," *Aerospace*, vol. 2, no. 4, pp. 555–580, Dec. 2015, doi: 10.3390/aerospace2040555.

[40] Z. Liu, G. Huang, J. Chen, and Z. Yu, "Coupling Effect between Inlet Distortion Vortex and Fan," *Journal of Thermal Science*, vol. 32, no. 3, pp. 1089–1104, May 2023, doi: 10.1007/s11630-023-1780-4.

[41] S. Deng, S. Wang, and Z. Zhang, "Aerodynamic performance assessment of a ducted fan UAV for VTOL applications," *Aerosp Sci Technol*, vol. 103, Aug. 2020, doi: 10.1016/j.ast.2020.105895.

7   APPENDIX

MATLAB Code for Blade Design

```matlab
thrust = 88964;                         %Newtons

dia = 1.27;                             %m

r = dia/2;

%Power = 5178415.662;                   %Joules/s 204 kg/s ICASE

rho_in = 1.225;                         %kg/m3

P_in = 101325;                          %Pa

cp = 1005;

T_in = 298;                             %K

R = 287;                                %Gas Constant

vel_in = 204;                           %0.6 Mach

m_dot = 204;                            %mass flow rate

dh = sqrt((dia^2)-((4*m_dot)/(rho_in*pi*vel_in)));

A_1 = pi*((1.27/2)^2-(dh/2)^2);

del_P = thrust/A_1;                     %Pressure out%

P_out = P_in+del_P;                     %Pressure difference%

PR = P_out/P_in;

u1 = vel_in/r;                          %rad/s %for 0.6 mach i.e
205.8 m/s

u = u1*(dh/2);                          %m/s

u_tip = u1*(dia/2);

RPM = (u1*60)/(2*pi);                   %omega to RPM for 0.6
Mach number%

del_h = (1/rho_in)*del_P;               %Enthalpy change%

del_T = del_h/cp;                       %Temperature difference%

T_out = del_T+T_in;                     %Temperature out%
```

```matlab
rho_out = P_out/(R*T_out);              %Density out%

%m_dot = Power/(cp*del_T);              %mass flow rate


cx1 = m_dot/(rho_in*A_1);               %velocity in

cx2 = m_dot/(rho_out*A_1);              %velocity out

%d_hub = sqrt(dh);                      %hub diameter

blade_l = (dia/2)-(dh/2);                   %tip dia

ratio_h_s = dh/dia;                     %hub to tip ratio

z = (6*ratio_h_s)/(1-ratio_h_s);        %number of blades

rm = ((dh/2)+(dia/2))/2;

s = (2*pi*rm)/z;                        %spacing

head = del_P/rho_out;

si = head/(u^2);

sigmas = cx1/cx2;                       %duct diffusion ratio

%%%%%%%%%%%%%%%%%%%%%%%%%%%%%%%%%%%%%%%%%%%%%%%%%%%%%%%%%%%%%%%
%%%%%%%%%%%%%
beta_1= atand(u/cx1);

w_1 = sqrt(cx1^2+u^2);

phi = cx2/u_tip;                        %flow coefficient

beta_2 = atand((1/phi)-(si/(4*phi)));

cy2 = del_h/(2*u);                      % cy3 = cy2

cy2_l = u-cy2;

u_3 = (2*u)-cy2_l;

beta_3 = atand(u_3/cx1);

w_3 = sqrt(cx1^2+u_3^2);                % 3 tangential

w_2 = atand(cy2_l/cx1);

beta_4 = atand(u/cx1);

w_4 = sqrt(cx1^2+u^2);
```

```matlab
cx4 = sqrt((w_4^2)-(u^2));

bZ = (2*pi*(dia/2))/s;

stagger = atand(u_tip/vel_in);

stages = (si*u^2)/cp;
```

MATLAB Code for Blade Profile Design

```matlab
% Define the angle parameters (in radians)
a1 = pi/6;   % Example value for a1 (30 degrees)
a2 = pi/3;   % Example value for a2 (60 degrees)

% Compute the control points for the B?zier curve
P0x = 0;
P0y = 0;

P1x = 1 / (1 + (cot(a1) / cot(a2)));
P1y = cot(a1) / (1 + (cot(a1) / cot(a2)));

P2x = 1;
P2y = 0;

% Number of points to plot the curve
numPoints = 100;

% Preallocate arrays for the curve points
B_x_suction = zeros(0, numPoints);
B_y_suction = zeros(0, numPoints);
B_x_pressure = zeros(0, numPoints);
B_y_pressure = zeros(0, numPoints);

% Parameter t ranges from 0 to 1
t = linspace(0, 1, numPoints);

% Compute the quadratic B?zier curve points for suction and
pressure sides
for i = 1:numPoints
    B_x_suction(i) = (1-t(i))^2 * P0x + 2*(1-t(i))*t(i) * P1x
+ t(i)^2 * P2x;
    B_y_suction(i) = (1-t(i))^2 * P0y + 2*(1-t(i))*t(i) * P1y
+ t(i)^2 * P2y;

    B_x_pressure(i) = (1-t(i))^2 * P0x + 2*(1-t(i))*t(i) * P1x
+ t(i)^2 * P2x;
    B_y_pressure(i) = (1-t(i))^2 * P0y + 2*(1-t(i))*t(i) * P1y
+ t(i)^2 * P2y;
end

% Calculate the suction and pressure side coordinates
```

```matlab
t_val = 0.1; % Example value for thickness
theta = atan2(P1y - P0y, P1x - P0x); % Calculate angle of the
line segment

x_c = (B_x_suction + B_x_pressure) / 2;
y_c = (B_y_suction + B_y_pressure) / 2;

xss = x_c - (t_val / 2) * sin(theta);
yss = y_c + (t_val / 2) * cos(theta);

xps = x_c + (t_val / 2) * sin(theta);
yps = y_c - (t_val / 2) * cos(theta);

% Plot the control points
figure;
plot(P0x, P0y, 'ro', 'MarkerSize', 10, 'DisplayName', 'P0');
hold on;
plot(P1x, P1y, 'go', 'MarkerSize', 10, 'DisplayName', 'P1');
plot(P2x, P2y, 'bo', 'MarkerSize', 10, 'DisplayName', 'P2');

% Plot the control polygon
plot([P0x, P1x, P2x], [P0y, P1y, P2y], 'k--', 'DisplayName',
'Control Polygon');

% Plot the B?zier curves for suction and pressure sides
plot(B_x_suction, B_y_suction, 'b-', 'LineWidth', 2,
'DisplayName', 'Bezier Curve (Suction Side)');
plot(B_x_pressure, B_y_pressure, 'r-', 'LineWidth', 2,
'DisplayName', 'Bezier Curve (Pressure Side)');

% Plot the suction and pressure sides
plot(xss, yss, 'm-', 'LineWidth', 2, 'DisplayName', 'Suction
Side');
plot(xps, yps, 'c-', 'LineWidth', 2, 'DisplayName', 'Pressure
Side');

% Add labels and legend
xlabel('x');
ylabel('y');
title('Quadratic Bezier Curve with Suction and Pressure
Sides');
legend('Location', 'Best');
grid on;
axis equal;
hold off;
```